PREPARATION, CHARACTERIZATION AND UTILIZATION AS SUPPORT MATERIALS FOR CATALYSTS CONTAINING PLATINUM AND IRON OF RH-MCM-41 AND RH-AlMCM-41

JITLADA   CHUMEE

A Thesis Submitted in Partial Fulfillment of the Requirements for the

Degree of Doctor of Philosophy in Chemistry

Suranaree University of Technology

Academic Year 2008

การเตรียม วิเคราะห์ลักษณะ และการใช้เป็นตัวรองรับตัวเร่งปฏิกิริยาแพลทินัม

และโลหะเหล็กของ RH-MCM-41 และ RH-AlMCM-41

นางสาวจิตรลดา ชูมี

PREPARATION, CHARACTERIZATION AND UTILIZATION AS SUPPORT MATERIALS FOR CATALYSTS CONTAINING PLATINUM AND IRON OF RH-MCM-41 AND RH-AlMCM-41
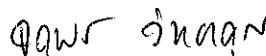
Suranaree University of Technology has approved this thesis submitted in partial fulfillment of the requirements for the Degree of Doctor of Philosophy.

Thesis Examining Committee

_____

(Assoc. Prof. Dr. Malee Tangsathitkulchai)

Chairperson

_____

(Assoc. Prof. Dr. Jatuporn Wittayakun)

Member (Thesis Advisor)

_____

(Assoc. Prof. Dr. Nurak Grisdanurak)
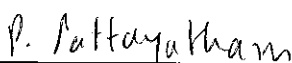
Member

_____

(Asst. Prof. Dr. Chaiwat Ruksakulpiwat)

Member

_____

(Dr. Sanchai Prayoonpokarach)

Member

_____　　　　_____

(Prof. Dr. Pairote Sattayatham)　　　　(Assoc. Prof. Dr. Prapan Manyum)

Vice Rector for Academic Affairs　　　　Dean of Institute of Science

จิตรลดา ชูมี : การเตรียม วิเคราะห์ลักษณะ และการใช้เป็นตัวรองรับตัวเร่งปฏิกิริยา
แพลทินัมและโลหะเหล็กของ RH-MCM-41 และ RH-AlMCM-41 (PREPARATION,
CHARACTERIZATION AND UTILIZATION AS SUPPORT MATERIALS FOR
CATALYSTS CONTAINING PLATINUM AND IRON OF RH-MCM-41 AND
RH-AlMCM-41) อาจารย์ที่ปรึกษา : รองศาสตราจารย์ ดร. จตุพร วิทยาคุณ, 100 หน้า.

เป้าหมายของวิทยานิพนธ์นี้ คือการนำแกลบข้าวซึ่งเป็นวัสดุเหลือใช้จากการสีข้าว มาใช้
ประโยชน์ โดยนำมาสกัดด้วยกรดเพื่อผลิตซิลิกาสันฐานที่มีความบริสุทธิ์สูงสำหรับเป็นสารตั้งต้น
ในการสังเคราะห์วัสดุมีโซพอรัส RH-MCM-41 ด้วยวิธีไฮโดรเทอร์มัล หลังจากการวิเคราะห์
ลักษณะตัวอย่างที่สังเคราะห์ได้ด้วยเทคนิคการเลี้ยวเบนรังสีเอกซ์ การดูดซับด้วยแก๊สไนโตรเจน
และกล้องจุลทรรศน์อิเล็กตรอนแบบส่องผ่าน พบว่ามีโครงสร้างผลึกแบบเฮกซะโกนัล มีพื้นที่ผิว
สูง มีการจัดเรียงตัวอย่างเป็นระเบียบ และมีความเสถียรกว่าการสังเคราะห์ RH-MCM-41 ที่สภาวะ
ปรกติ เนื่องจากผนังมีความหนามากกว่า หลังจากนั้นทำการดัดแปรเพื่อเพิ่มความเป็นกรด ด้วยการ
เติมอะลูมิเนียมไปบน RH-MCM-41 ที่สังเคราะห์ไว้แล้ว เพื่อผลิต RH-AlMCM-41 หลังจากการ
เติมอะลูมิเนียมพบว่าพื้นที่ผิวลดลงแต่ยังคงโครงสร้างผลึกแบบเฮกซะโกนอล จากนั้นนำทั้ง RH-
MCM-41 และ RH-AlMCM-41 ไปเป็นตัวรองรับสำหรับตัวเร่งปฏิกิริยาโลหะผสมระหว่างเหล็ก
(Fe) และแพลทินัม (Pt) โดยตัวเร่งปฏิกิริยาที่เตรียมมีปริมาณ Fe เท่ากับ 5% โดยน้ำหนักและ
ปริมาณ Pt เท่ากับ 0.5% โดยน้ำหนัก หลังจากเติมโลหะลงบน RH-MCM-41 และ RH-AlMCM-41
พบว่า ความเป็นผลึกและพื้นที่ผิวมีค่าลดลง โลหะ Fe ที่เติมลงไปมีเลขออกซิเดชันเป็น +3 อยู่ใน
ลักษณะของเหล็กออกไซด์

เมื่อนำ   5Fe0.5Pt/RH-MCM-41   ไปทดสอบการเร่งปฏิกิริยาการเติมหมู่ไฮดรอกซิลบน
ฟีนอล โดยใช้ไฮโดรเจนเปอร์ออกไซด์ เพื่อผลิตแคทิคอลและไฮโดรควิโนน ที่อุณหภูมิ 70 องศา
เซลเซียส โดยแปรอัตราส่วนโดยโมลระหว่างฟีนอลกับไฮโดรเจนเปอร์ออกไซด์เป็น 2:1 1:2 2:3
และ 2:4 พบว่า ที่อัตราส่วน 2:4 ให้ค่าการแปรผันสูงสุด แต่มีผลิตภัณฑ์ซึ่งไม่ต้องการ คือ เบนโซควิ
โนนเพิ่มขึ้นมา   สามอัตราส่วนแรกให้ผลิตภัณฑ์ที่เป็นแคทิคอลและไฮโดรควิโนนเท่านั้น   และ
อัตราส่วนระหว่างฟีนอลกับไฮโดรเจนเปอร์ออกไซด์ที่เหมาะสมที่สุดคือ 2:3 เพราะให้ค่าการแปร
ผันสูง   เมื่อเปรียบเทียบค่าการแปรผันของฟีนอลกับตัวเร่งปฏิกิริยาที่เตรียมจากตัวเร่งปฏิกิริยาที่
เตรียมจากการผสมระหว่าง 0.5Pt/RH-MCM-41 กับ 5Fe/RH-MCM-41 และ 5Fe0.5Pt/RH-Silica
พบว่า ตัวเร่งปฏิกิริยา 5Fe0.5Pt/RH-MCM-41 มีค่าการแปรผันสูงกว่าเป็นการยืนยันว่าการเตรียม

ตัวเร่งปฏิกิริยาที่เตรียมจากการใส่โลหะสองตัวเข้าไปพร้อมกัน และการกระจายตัวของโลหะบนตัว
รองรับ RH-MCM-41 มีพื้นที่ผิวสูงกว่าซิลิกา ทำให้เร่งปฏิกิริยาได้ดีขึ้น ส่วนการเร่งปฏิกิริยาของ
PtFe/RH-AlMCM-41 ที่อัตราส่วนโดยโมลระหว่างฟีนอลกับไฮโดรเจนเปอร์ออกไซด์เป็น 2:3
เท่านั้น พบว่าให้ผลิตภัณฑ์ที่เป็นเพียงแคทิคอลและไฮโดรควิโนนเท่านั้น แต่ค่าการแปรผันของ
ฟีนอลบนตัวเร่งปฏิกิริยานี้มีค่าน้อยกว่า PtFe/RH-MCM-41 เนื่องจากตัวเร่งปฏิกิริยาอยู่บนตัว
รองรับที่มีพื้นที่ผิวน้อยกว่าเนื่องจากการเติมอะลูมิเนียม

สาขาวิชาเคมี   ลายมือชื่อนักศึกษา_____

ปีการศึกษา 2551   ลายมือชื่ออาจารย์ที่ปรึกษา_____

JITLADA CHUMEE : PREPARATION, CHARACTERIZATION AND
UTILIZATION AS SUPPORT MATERIALS FOR CATALYSTS
CONTAINING PLATINUM AND IRON OF RH-MCM-41 AND
RH-ALMCM-41. THESIS ADVISOR : ASSOC. PROF. JATUPORN
WITTAYAKUN, Ph.D. 100 PP.

RH-MCM-41/PLATINUM/IRON/PHENOL HYDROXYLATION/RICE HUSK

The goal of this thesis was to extract amorphous and high purity silica from rice husk, a by-product from rice milling, and used as a silica source for the synthesis of mesoporous material RH-MCM-41 by hydrothermal method. Characterizations by X-ray diffraction (XRD), N_2 adsorption and transmission electron microscopy (TEM) indicated that the RH-MCM-41 still had a hexagonal lattice, high surface area and well-ordered structure. The RH-MCM-41 synthesized by hydrothermal was more stable than RH-MCM-41 synthesized with ambient conditions because the pore walls were thicker. The RH-MCM-41 was modifies further by adding aluminium on the preformed RH-MCM-41 to produced RH-AlMCM-41. The modified RH-MCM-41 had lower surface area but still contained the hexagonal structure of RH-MCM-41. Both RH-MCM-41 and RH-AlMCM-41 were used as support materials for platinum (Pt) and iron (Fe) catalysts that the loading of Fe and Pt were 5 and 0.5%wt, respectively. After metal addition, the crystallinity of the supports decreased and the oxidation state of Fe was +3 in oxide form.

The 5Fe0.5Pt/RH-MCM-41 was tested for phenol hydroxylation by using H_2O_2 solution at 70 °C with the phenol: H_2O_2 mole ratio of 2:1, 2:2, 2:3 and 2:4 to produce catechol and hydroquinone. The ratio 2:4 gave the highest phenol conversion an undesired by-product, benzoquinone, was produced. The first three ratios gave only catechol and hydroquinone with the highest conversion on the phenol: H_2O_2 mole ratio of 2:3. The phenol conversion on 5Fe0.5Pt/RH-MCM-41 was higher than that of a physical mixture between 0.5Pt/RH-MCM-41 and 5Fe/RH-MCM-41, and higher than that of 5Fe0.5Pt/RH-Silica indicating that the effective catalyst can be prepared by co-impregnation of Fe and Pt on the same support. The improvement is also achieved by the metal dispersion on RH-MCM-41 which has a higher surface area than the RH-Silica. The catalytic performance of 5Fe0.5Pt/RH-MCM-41 was better than that of 5Fe0.5Pt/RH-AlMCM-41 which was only tested with the phenol: H_2O_2 mole ratio of 2:3 because the RH-MCM-41 support had a significantly higher surface area than the RH-AlMCM-41.

School of Chemistry   Student's Signature_____

Academic Year 2008   Advisor's Signature_____

ACKNOWLEDGEMENT

Jitlada Chumee

CONTENTS

CONTENTS (Continued)

CONTENTS (Continued)

CONTENTS (Continued)

LIST OF FIGURES

LIST OF FIGURES (Continued)

LIST OF FIGURES (Continued)

LIST OF TABLES

LIST OF TABLES (Continued)

LIST OF SCHEME

CHAPTER I

INTRODUCTION

This thesis includes synthesis and characterization of mesoporous material known as MCM-41 using silica from rice husk which can be considered as an abundant solid waste from milling process. This utilization of rice husk silica is an alternative way to increase the rice husk value. The obtained MCM-41, referred throughout this thesis as RH-MCM-41 was further modified to increase acidity by Al addition to produced Al-RH-MCM-41 with different Si/Al ratio by post-synthetic grafting method (Post). Both RH-MCM-41 and Al-RH-MCM-41 were used as support materials for catalysts containing platinum (Pt) and iron (Fe). The literature reviews of MCM-41, modification and utilization are provided in Chapter II.

The chemical and physical properties of the supports and catalysts were investigated by several techniques including nitrogen adsorption-desorption analysis to obtain adsorption isotherm, BET surface area and pore size diameter, transmission electron microscopy (TEM) to observe material morphology, powder X-ray diffraction (XRD) to determine the phase and crystallinity of materials and to confirm the formation of MCM-41 framework, X-ray fluorescence (XRF) to determine the elemental composition, extended X-ray absorption fine structure (EXAFS) and X-ray absorption near edge structure (XANES) to investigate environment and oxidation state of Fe catalysts.

Finally, the monometallic and bimetallic catalysts were tested for phenol hydroxylation in a batch reactor under various reaction conditions. The reactants and products from the reaction were analyzed by gas chromatography (GC).

1.1   Research objectives

1. To prepare and characterize RH-MCM-41 using rice husk silica.

2. To modify RH-MCM-41 to increase acidity by Al addition with post-synthetic grafting method (Post) and characterize the obtained Al-MCM-41 to observe changes after modification.

3. To prepare and characterize bimetallic catalysts containing platinum and iron supported on RH-MCM-41 and RH-AlMCM-41.

4. To test the bimetallic catalysts for phenol hydroxylation

5. To study effect of parameters such as mole ratios of phenol:H_2O_2 and temperature in order to find optimum conditions.

1.2   Scope and limitation of the study

1. RH-MCM-41 was prepared from rice husk silica by a method modified from literatures.

2. Aluminium addition was conducted by post-synthetic grafting method (Post) with Si/Al ratio equal to 75 and 25.

3. Catalysts containing platinum and iron were prepared by co-impregnation techniques.

4. The catalysts and support were characterized by various techniques including BET, TEM, XRD, XRF, FT-IR, EXAFS and XANES.

5. The reaction for testing all catalysts was phenol hydroxylation in a batch reactor at 70 °C with various mole ratio of phenol:H_2O_2.

6. The reactants and products from reaction were only analyzed by gas chromatography (GC).

CHAPTER II

LITERATURE REVIEW

2.1 Background of rice husk silica

Rice husk is the rice milling byproduct that can be considered as a solid waste in the agricultural industry (Tsay and Chang, 2000). The major constituents of rice husk are organic compounds, mainly cellulose and lignin and inorganic compounds, mainly silica. The husk compositions vary with geographic location and climate. After burning rice husk, the obtained ash composes of silica with small amounts of other inorganic compounds such as oxides of aluminum, iron, calcium. Silica with high purity can be obtained from rice husk by leaching with acids and calcination at 600 °C under a static air or flowing atmosphere (Yalçin and Sevinç, 2001). Among several types of acid, HCl is often used as a leaching agent. The silica from rice husk could be used as a source for preparation of a number of silicon compounds such as silicon carbide, silicon nitride, zeolite and mesoporous MCM-41. (Sun and Gong, 2001; Huang et al., 2001; Krishnarao et al., 2001) This thesis focuses on using rice husk silica as a source for the synthesis of mesoporous material, referred to as RH-MCM-41 througout this thesis.

2.2 Background of MCM-41 and Al-MCM-41

Mesoporous MCM-41 is an amorphous silica with a regular pore system consisting of an array of unidimensional and hexagonally shaped mesopores (pore size range of 2-50 nm). The pore size of the MCM-41 can be controlled by use of

appropriate surfactants with various chain lengths as templates. Because of its uniform size and shape of mesopores as well as thermal stability, MCM-41 is interesting as a model substance for gas adsorption, catalyst support (Matsumoto et al., 1999). MCM-41 was originally synthesized by hydrothermal reactions of silicate gels at the temperature of 100-120 °C (Shylesh and Singh, 2004). Like amorphous silica, surface of the MCM-41 is only weakly acidic. Acidity modification of MCM-41 is necessary for the applications to acid-catalyzed reactions such as cracking, isomerization, alkylation and hydroxylation (Matsumoto et al., 1999; Shylesh and Singh, 2004; Park et al., 2002). An introduction of tetrahedrally coordinated aluminum (T_d-Al) into its structure can create Brønsted acid sites. In addition, the acidity of MCM-41 can be generated by isomorphous substitution of Si by Al. There were two methods to introduce Al to MCM-41: a direct sol–gel method (Pre) and a post-synthetic grafting method (Post). The Pre-method produced Al-containing within the MCM-41 structure denoted Al-MCM-41 but its structure was not hydrothermally stable (Park et al., 2002). The Al-MCM-41 had very low concentration and strength of Brønsted acid sites even at high aluminum content. Therefore, the post-synthetic modifications have been developed to maintain structural stability and to make it easy to incorporate various metal elements into siliceous MCM-41 support (Park et al., 2002). In this work, MCM-41 and Al-MCM-41 from post-synthetic modification are prepared and used as catalyst supported materials.

2.3 Background of phenol hydroxylation

Catalytic oxidation processes are interesting because they can be used industrially in the production of fine chemicals. Organic compounds such as olefins,

amines, and aromatics can be transformed by using redox molecular sieves as catalysts with H_2O_2 in aqueous solution as the oxidant without producing environmentally unfriendly side products (Jing et al., 2002). Redox molecular sieves are promising materials for transformations of large organic molecules in liquid phase reactions because they can incorporate various transition metal species such as Ti, V, Fe, Zr, Mn, Pd, Pt and Sn into the mesoporous silica hosts materials. Large surface areas of these materials coupled with uniform mesopores in large pore volume are envisaged to be useful in promoting high dispersion of active sites and in enhancing diffusion rates of reactants/products in liquid phase reactions (Choi et al., 2006; Kuznetsova et al., 2005).

Hydroxylation of phenol by reaction with hydrogen peroxide to produce dihydroxybenzenes (Figure 2.1) is an important selective oxidation. The products, catechol and hydroquinone, are useful in the production of various compounds such as photographic chemicals, antioxidants, flavoring agents, polymerization inhibitors and pharmaceuticals (Kannan et al., 2005). Phenol hydroxylation with 30% H_2O_2 would be a useful process because of its simplicity and lack of by-product pollutants.
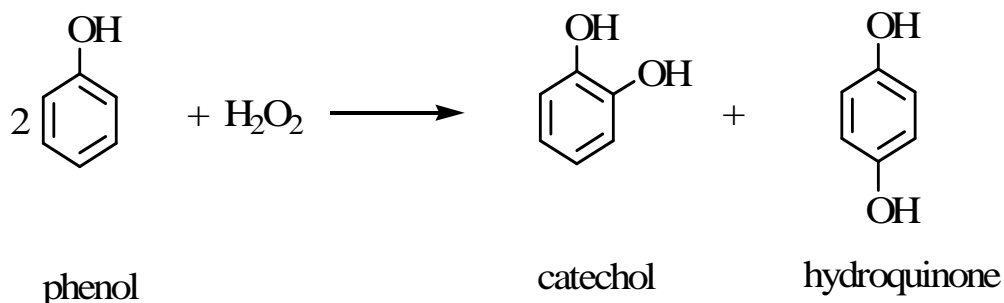
Figure 2.1 Hydroxylation of phenol.

The phenol conversion could not occur without a catalyst indicating that the acid site and metal catalysts are required for the reaction. This work focused on phenol hydroxylation on bimetallic platinum-iron catalysts supported on RH-MCM-41 and Al-RH-MCM-41. Platinum and iron catalysts are interesting because they are widely used in many reactions of organic compounds such as decomposition, alkylation, hydrogenation, dehydrogenation, selective oxidation and hydroxylation (Matsumoto et al., 1999; Shylesh and Singh, 2004; Park et al., 2002). Because the pore size of MCM-41 is larger than pore size of zeolite, phenol can adsorb more easily. Furthermore, the generation of acid sites with Al addition should further improve the adsorption. Reviews on related works are summarized below.

2.4 Background of phenol hydroxylation catalyzed by platinum and iron

Table 2.1 shows examples of catalysts for phenol hydroxylation, conditions and % phenol conversion. The phenol oxidation on Pt catalysts supported on graphite in a stirred tank reactor was studied and the selectivity of the oxidation products depended on the degree of oxygen coverage on platinum surface (Masende et al., 2006). As shown in Figure 2.2, the over-oxidised platinum was proposed to be favorable for the formation of hydroquinone whereas the partially oxidized platinum was proposed to be favorable for the formation of catechol. The phenol hydroxylation on Fe catalysts was also reported for various supports, temperature and phenol:H_2O_2 ratios (Choi et al., 2006; Wu et al., 2008; Preethi et al., 2008; Liu et al., 2008; Hao et al., 2001; Letaïëf et al., 2008;. Mohamed et al., 1993; Abbo et al., 2005).

Table 2.1 Examples of catalysts, condition and % conversion of phenol for hydroxylation of phenol.

Catalyst	Temperature, solvent	phenol:H_2O_2	% conversion of phenol	Reference
none	60 °C, water	1:1	0.0	Jun et al.
NaY			1.7	(2004)
CuNaY			51.1	
TS-1	50 °C, acetone	3:1	1.27	Liu et al. (2006)
Fe-Co-NaY	70 °C, water	3:1	21.8	Park et al. (2006)
Fe-ZSM-5	80 °C, water	3:1	32.9	Villa et al. (2005)
CuO–MCM-48	80 °C, water	3:1	29.5	Lou and Liu (2005)
Fe-MCM-41	50 °C, water	1:1	60.0	Choi et al. (2006)
Pt/graphite	150 °C, water	3.1	25.0	Masende et al. (2003)

TS-1= titanium silicalite-1
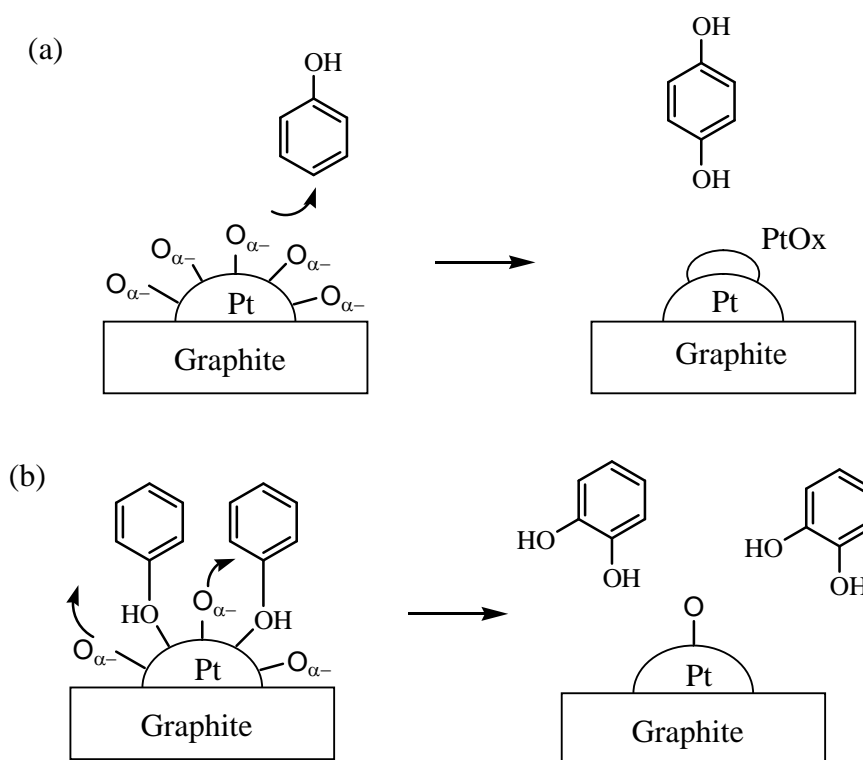
Figure 2.2 Proposed mechanism of phenol hydroxylation by attacking of phenol by OH radical or oxygen insertion on (a) by dehydrogenation or dehydroxylation over-oxidesed Pt supported on carbon and (b) partly oxidized surface (Masende et al., 2006).

Table 2.2 shows examples of phenol hydroxylation on various catalysts and conditions. The highest conversion of 60% was obtained on Fe/MCM-41 with ~10 wt% Fe at 70 °C with the phenol:H_2O_2 ratio of 1:1 (Choi et al., 2006). The reaction mechanism with H_2O_2 solution over Fe/MCM-41 was also proposed that Fe^{3+} reacted with H_2O_2 to form OH radicals which reacted with phenol to form catechol and hydroquinone. In addition, the phenol conversion of 58.5% was obtained from Fe/Al-MCM-41 catalyst with 10 wt% Fe at 40 °C (Preethi et al., 2008).

Preethi et al. (2008) synthesized Al-MCM-41 by hydrothermal method with the Si/Al ratio of 25, 50, 75 and 100 and impregnated them with iron precursor to give 10%Fe/Al-MCM-41. The materials and characterized by the XRD, nitrogen adsopion-desorption analysis, FT-IR, and UV- vis and Mössbauer techniques. The liquid phase hydroxylation with the phenol:H_2O_2 ratio of 1:3 was studied. The phenol conversion was found to be almost the same (~60%) at 40, 60 and 80 °C, but about only 30% at room temperature. The activity depended on the support acidity in the following order: Fe/Al-MCM-41(25) > Fe/Al-MCM-41(50) > Fe/Al-MCM-41(75) > Fe/Al-MCM-41(100), where the number in parentheses are Si/Al ratios.

Wu et al. (2008) synthesized Fe/MCM-41s catalysts by hydrothermal method and characterized by XRD, BET, HRTEM, FT-IR, UV-vis and ICP techniques. The iron species were mainly in the framework with isolated tetrahedral coordination and micro-crystals of Fe_2O_3. Their catalytic performances for phenol hydroxylation with the phenol:H_2O_2 ratio of 3:1 were studied. Results indicated that the mesoporous structure did not collapse and the prepared samples exhibited excellent catalytic activities for phenol hydroxylation by H_2O_2 at room temperature with about 16% conversion.

Zhao et al. (2000) synthesized highly ordered Fe-MCM-48 by a mixed templation method under low molar ratio (0.17: 1) of mixed surfactants to silica and characterized by XRD, ^{29}Si-MAS NMR, ESR, and UV-Visible. Its catalytic activity and selectivity was studied for phenol hydroxylation using H_2O_2 (30%). The

substituting element (Fe^{3+}) is partially incorporated into the framework position forming a new type of active site which raises the phenol conversion to 43.6%

Table 2.2 Examples of Fe catalysts, condition and % conversion of phenol for hydroxylation of phenol to produce catechol (CE) and hydroquinone (HQ)

Catalyst, preparation of catalyst	Conditions, phenol:H_2O_2 ratio and catalyst amount	% Phenol conversion	Selectivity		Ref.
			CE	HQ	
8% mole Fe/MCM-41, gel composition	30 °C, 2 h, 3:1, water, 0.05 g	16	78	19	Wu et al. (2008)
4%mole Fe/MCM-41, gel composition	50 °C, 1 h, 1:1, water, 0.03 g	60.0	68	32	Choi et al. (2006)
0.153% mole Fe/MCM-48, gel composition	60 °C, 4 h, 1:1, water, 0.01 g	43.6	73.3	24.4	Zhao et al. (2000)
10 wt% Fe/AlMCM-41, wet impregnation	40 °C, 4 h , 1:3, water, 0.1 g	58.5	38.0	61.0	Preethi et al. (2008)
2 wt% Fe/NaY, ion exchange	70 °C, 4 h , 3:1, water, 2 g	21.8	44.8	16.5	Park et al. (2006)

Choi et al. (2006) synthesized a highly ordered iron-containing mesoporous material, Fe-MCM-41, with 0.5 - 4 mole Fe/Si ratio and characterization by using XRD, SEM/TEM, EDS, N_2-sorption, and FT-IR and UV–vis spectroscopies. Fe-MCM-41 exhibited high catalytic activity in phenol hydroxylation using H_2O_2 as oxidant, giving phenol conversion 60% at 50 °C [phenol:H_2O_2 = 1:1, water solvent].

$$Fe^{3+} + H_2O_2 \rightleftharpoons Fe^{2+} + \bullet OOH + H^+$$

$$Fe^{2+} + H_2O_2 \rightleftharpoons Fe^{3+} + \bullet OH + OH^-$$
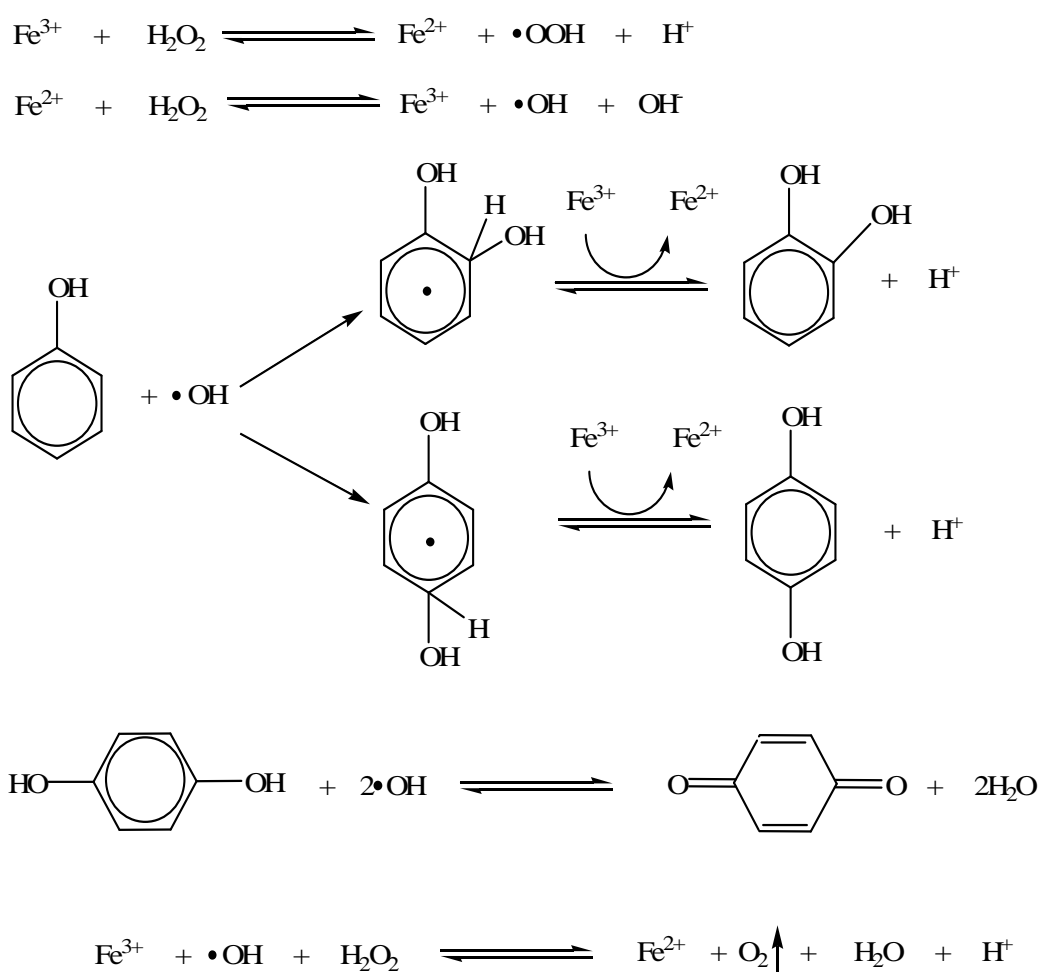
Figure 2.3 Proposed mechanism of phenol hydroxylation with H_2O_2 solution over Fe/MCM-41 (Choi et al., 2006).

Park et al. (2006) prepared Fe-NaY, Co-NaY and Fe-Co-NaY catalysts by ion-exchange of NaY through the wet method. Their catalytic performances for the phenol hydroxylation were evaluated between 30 and 90 °C. The Fe-Co-NaY catalyst showed a higher activity than either Fe-NaY or Co-NaY catalysts. The optimum conditions were 70 °C, phenol:H_2O_2 of 3:1 and water solvent, 21.8% phenol conversion was obtained with 44.8% selectivity to catechol, and 16.5% to hydroquinone.

A proposed mechanism of phenol hydroxylation with H_2O_2 solution over Fe/MCM-41 showed in Figure 2.3 that the Fe^{3+} sites reacted with H_2O_2 to form hydroxyl radicals which reacted with phenol to form catechol and hydroquinone (Choi et al., 2006).

In this work, platinum and iron supported on RH-MCM-41 and RH-AlMCM-41 were used as catalysts in hydroxylation of phenol.

2.5 References

Abbo, H. S., Titinchi, S. J., Prasad, R. and Hand, S. (2005). Synthesis, characterization and study of polymeric iron(III) complexes with bidentate *p*-hydroxy Schiff bases as heterogeneous catalysts. **Journal of Molecular Catalysis A: Chemical** 225: 225-232.

Chiarakorn S., Areerob T. and Grisdanurak N. (2007). Influence of functional silanes on hydrophobicity of MCM-41 synthesized from rice husk. **Science and Technology of Advanced Materials** 8: 110-115.

Choi, J., Yoon, S., Jang, S. and Ahn, W. (2006). Phenol hydroxylation using Fe-MCM-41 catalysts. **Catalysis Today** 111: 280-287.

Grisdanurak, N., Chiarakorn, S. and Wittayakun, J. (2003). Utilization of mesoporous molecular sieve synthesized from natural source rice husk silica to chlorinated volatile organic compounds (CVOCS) adsorption. **Korean Journal of Chemical Engineering** 20: 950-955.

Hao, W., Luo, Y., Deng, P. and Li, Q. (2001). Synthesis of Fe-MCM-48 and its catalytic performance in phenol hydroxylation. **Catalysis Letters** 73: 199-202.

Huang, S., Jing S., Wang, J., Wang, Z. and Jin, Y. (2001). Silica white obtained from rice husk in fluidized bed. **Powder Technology** 117: 232-238.

Jermy R. B. and Pandurangan A. (2005)**.** Catalytic application of Al-MCM-41 in the esterification of acetic acid with various alcohols. **Applied Catalysis A: General** 288: 25-33.

Jia, J., Shen, J., Lin, L., Xu, Z., Zhang, T. and Liang, D. (1999). A study on reduction behaviors of the supported platinum-iron catalysts. **Journal Molecular Catalysis A: Chemical** 138: 177-184.

Jia, Y., Han, W., Xiong, G. and Yang, W. (2007) Diatomite as high performance and environmental friendly catalysts for phenol hydroxylation with H_2O_2. **Science and Technology of Advanced Materials** 8: 106-109.

Jing, H., Guo, Z., Ma, H., Evans D. G. and Duan X. (2002). Enhancing the selectivity of benzene hydroxylation by tailoring the chemical affinity of the MCM-41 catalyst surface for the reactive molecules. **Journal of Catalysis** 212: 22-32.

Kannan, S., Dubey, A. and Knozinger, H. (2005). Synthesis and characterization of CuMgAl ternary hydrotalcites as catalysts for the hydroxylation of phenol. **Journal of Catalysis** 231: 381-392.

Khemthong, P., Wittayakun, J. and Prayoonpokarach, S. (2007). Synthesis and characterization of zeolite LSX from rice husk silica. **Suranaree Journal of Science and Technology** 14: 367-739.

Krishnarao, R. V., Subrahmanyam, J. and Jagadish Kumar T. (2001). Studies on the formation of black particles in rice husk silica ash. **Journal of the European Ceramic Society** 21: 99-104.

Kuznetsova, I. N., Kuznetsova, I. L., Likholobov, A.V. and Pez, P. G. (2005). Hydroxylation of benzene with oxygen and hydrogen over catalysts containing Group VIII metals and heteropoly compounds. **Catalysis Today** 99: 193-198.

Kordatos, K., Gavela, S., Ntziouni, A., Pistiolas, K.N., Kyritsi, A. and Kasselouri-Rigopoulou, V. (2008). Synthesis of highly siliceous ZSM-5 zeolite using silica from rice husk ash. **Microporous and Mesoporous Materials** 115: 189-196.

Park, J.-N., Wang, J., Choi, Y. K., Dong, W.-Y., Hong, S.-I. and Lee W. C. (2006). Hydroxylation of phenol with H_2O_2 over Fe^{2+} and/or Co^{2+} ion-exchanged NaY catalyst in the fixed-bed flow reactor. **Journal Molecular Catalysis A: Chemical** 247: 73-79.

Park, K.-C., Yim, D. and Ihm, S (2002). Characteristics of Al-MCM-41 supported Pt catalysts: effect of Al distribution in Al-MCM-41 on its catalytic activity in naphthalene hydrogenation. **Catalysis Today** 74:281-290.

Letaïef, S., Casal, B., Aranda, P., Martín-Luengo, M. A. and Ruiz-Hitzky, E. (2003). Fe-containing pillared clays as catalysts for phenol hydroxylation. **Applied Clay Science** 22: 263-277.

Liu, H., Lu, G., Guo, Y., Guo, Y. and Wang, J. (2008). Study on the synthesis and the catalytic properties of Fe-HMS materials in the hydroxylation of phenol. **Microporous and Mesoporous Materials** 108: 56-64.

Masende, G. P. Z., Kuster, M. F. B., Ptasinski, J. K., Janssen, G. J. J. F., Katima, Y. H. J. and Schouten C. J. (2003). Platinum catalysed wet oxidation of phenol in a stirred slurry reactor; The role of oxygen and phenol loads on reaction pathways. **Catalysis Today** 79-80: 357-370.

Matsumoto, A., Chen H., Tsutsumi, K., Grün, M. and Unger, K. (1999). Novel route in the synthesis of MCM-41 containing framework aluminum and its characterization. **Microporous Mesoporous Materials** 32: 55-62.

Ming-Tseh, T. and Feg-Wen, C. (2000). Characterization of rice husk ash-supported nickel catalysts prepared by ion exchange. **Applied Catalysis A** 203: 15-22.

Preethi, M. E. L., Revathi, S., Sivakumar, T., Manikandan, D., Divakar, D., Rupa, A. V. and Palanichami, M. (2008). Phenol Hydroxylation Using Fe/Al-MCM-41 Catalysts. **Catalysis Letters** 120: 56-64.

Shylesh, S. and Singh, P.A. (2004). Synthesis, characterization, and catalytic activity of vanadium-incorporated, -grafted, and -immobilized mesoporous MCM-41 in the oxidation of aromatics. **Journal of Catalysis** 228: 333-346.

Sun, L. and Gong, K. (2001). Silicon-based material from rice husks and their applications. **Industrial Engineering Chemistry Research** 40: 5861-5877.

Tang, H., Ren, Y., Bin, Y., Yan, S. and He, H. (2006). Cu-incorporated mesoporous materials: synthesis, characterization and catalytic activity in phenol hydroxylation. **Journal Molecular Catalysis A: Chemical** 260: 121-127.

Wittayakun, J., Khemthong, P., and Prayoonpokrach S. (2008). Synthesis and characterization of zeolite Y from rice husk silica. **Korean Journal of Chemical Engineering** 25: 861-864.

Wu, C., Kong, Y., Gao, F., Wu, Y., Lu, Y., Wang, J. and Dong, L. (2008). Synthesis, characterization and catalytic performance for phenol hydroxylation of Fe-MCM41 with high iron content. **Microporous and Mesoporous Materials** 113: 163-170.

Yalçin, N. and Sevinç V. (2001). Studies on silica obtained from rice husk. **Ceramics International** 27: 219-224.

Zhao, W., Luo, Y., Deng, P. and Li, Q. (2000). Synthesis of Fe-MCM-48 and its catalytic performance in phenol hydroxylation. **Catalysis Letters** 73: 2-4.

CHAPTER III

SYNTHESIS AND CHARACTERIZATION

OF RH-MCM-41

Abstract

The rice husk silica was prepared by acid leaching and characterized by X-ray diffraction (XRD) and X-ray fluorescence (XRF). The obtained product contained amorphous silica with purity of 98 wt% along with small amount of other inorganic compounds. The rice husk silica was used as silica source for the synthesis of MCM-41 which is a mesoporous material by hydrothermal gel method. The resulting product, notated as RH-MCM-41 was characterized by XRD, N_2 adsorption-desorption, transmission electron microscopy (TEM), Fourier transform infrared spectroscopy (FT-IR) and thermogravimetric analysis (TGA). The RH-MCM-41 XRD spectrum confirmed the MCM-41 characteristics. Its surface area was 1335 m^2/g and average pore size of 29 Å. The regular of hexagonal array morphology was observed by TEM and the FTIR confirmed functional groups. The RH-MCM-41 synthesized with rice husk silica by hydrothermal method was more stable than RH-MCM-41 synthesized with ambient conditions.

3.1 Introduction

Rice husk is a by-product from rice milling and could be considered as an agricultural waste. Because it consists of about 30 wt% of silica along with organic components, the silica with purity more than 98 wt% could be extracted from the husk by acid leaching and calcination (Khemthong et al., 2008). Rice husk silica has been used as a silica source for preparation of many silicon-containing compounds such as silicon carbide, silicon nitride, zeolite and mesoporous MCM-41 (Sun and Gong, 2001; Huang et al., 2001; Krishnarao et al., 2001).

This chapter focused on using rice husk silica in the synthesis of MCM-41 which would be referred to as RH-MCM-41. MCM-41 is amorphous silica with a regular mesopore system with the pore size in the range of 2-50 nm. Its structure consists of arrays of unidimensional and hexagonally shaped mesopores. The pore size of the MCM-41 can be controlled by use of an appropriate surfactant with a certain chain length as a template. Because of its uniform pore size and shape as well as its thermal stability, MCM-41 has attracted considerable interest for various applications especially as gas adsorbents and catalyst supports (Matsumoto et al., 1999; Grisdanurak et al., 2003; Chiarakorn et al., 2007). The RH-MCM-41 from rice husk silica synthesized under ambient conditions could be used effectively as adsorbents for chlorinated volatile organic compounds (Grisdanurak et al., 2003). Further modification to improve hydrophobicity of RH-MCM-41 from ambient synthesis could be carried out by silylation with silanes (Chiarakorn et al., 2007). However, it was believed that the MCM-41 synthesized at ambient conditions might

not be able to withstand harsh conditions. Thus, a hydrothermal gel method might improve the strength of the MCM-41 structure.

Details of this chapter includes an extraction of rice husk silica by acid leaching and characterization by powder X-ray diffraction (XRD) to confirm the phase of silica and X-ray fluorescence (XRF) to determine the elemental composition of silica. The obtained silica was used in the synthesis of RH-MCM-41 by hydrothermal gel method. The chemical and physical properties of the RH-MCM-41 were investigated by powder XRD to confirm the formation of RH-MCM-41 framework and to determine the phase and crystallinity. Its adsorption-desorption isotherm and surface area were obtained from the N_2 adsorption analysis. The morphology was investigated by transmission electron microscopy (TEM) and its functional groups were confirmed by Fourier transform infrared spectroscopy (FT-IR). In addition, changes and thermal stability of RH-MCM-41 during the template removal were studied by thermogravimetric analysis (TGA).

3.2 Experimental

3.2.1 Chemicals

The chemical for the extraction of rice husk silica was hydrochloric acid 37% (HCl) supplied by Carlo Erba. The chemicals for the synthesis of RH-MCM-41 were cetyltrimethyl ammonium bromide ($C_{16}H_{33}N(CH_3)_3Br$, CTAB) supplied by Fluka, sodium hydroxide, anhydrous pellet (NaOH) supplied by Carlo Erba, and concentrate sulphuric acid (96% H_2SO_4) supplied by Carlo Erba.

3.2.2 Extraction of rice husk silica and characterization

The rice husk was washed thoroughly with water to remove adhering soil and dust, dried at 120 °C overnight, mixed with 3 M HCl solution in ratio 100 g : 500 mL and refulxed in a round-bottom flask at 60 °C for 3 h. After filtration, the refluxed husk was washed with water several times until the filtrate was neutral, dried at 120 °C overnight in a hot-air oven and calcined at 500 °C for 6 h in a muffle furnace, with a heating ramp of 10 °C/min. The resulting white powder containing mainly silica (referred to as rice husk silica) was characterized by XRD and XRF.

3.2.3 Synthesis of RH-MCM-41

Rice husk silica was used as a silica source for the synthesis of RH-MCM-41 with a method modified from literature (Park et al., 2002). The procedure could be summarized in Scheme 3.1.
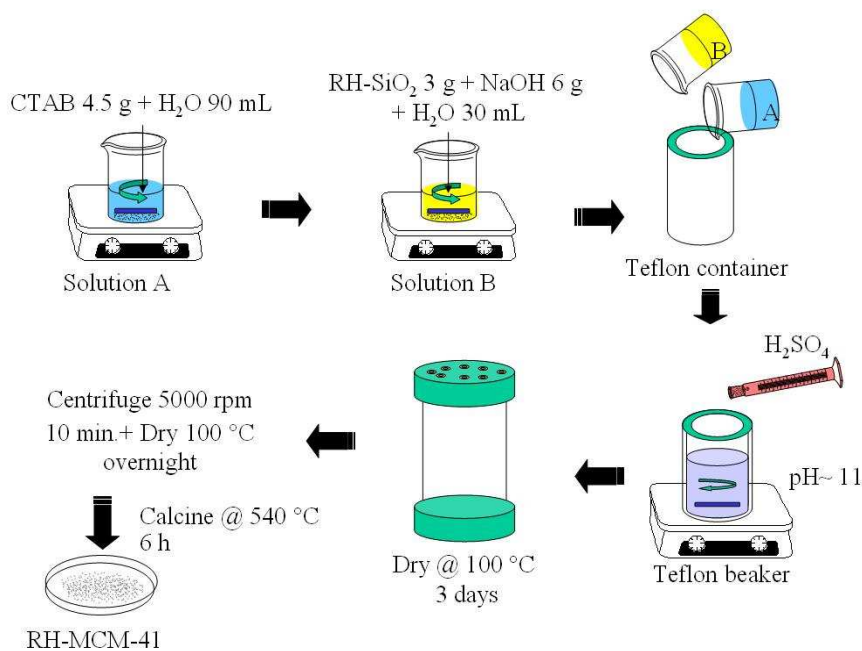
Scheme 3.1 Illustration of a synthetic procedure of RH-MCM-41.

A starting gel with a molar composition of $4SiO_2:1CTAB:0.29H_2SO_4:400H_2O$ was prepared in the following order. First, the rice husk silica (3 g) was dissolved in a 15 M of NaOH solution (10 mL). The obtained solution was then mixed with a 0.137 M CTAB solution and the pH of the gel mixture was adjusted to 11 with H_2SO_4. The gel mixture was stirred further for 2 h, transferred into a teflon-lined autoclave and kept at 100 °C under a static condition for 3 days. The solid material obtained was separated by centrifugation at 5000 rpm for 10 min, washed well with distilled water until the filtrate gave a neutral pH and dried in a hot air oven at 100 °C overnight. Finally the resulting material referred to as as-synthesized RH-MCM-41 was calcined at 540 °C in a muffle furnace for 6 h, at a heating ramp of 10 °C/min. The as-synthesized RH-MCM-41 was characterized by TGA and the calcined RH-MCM-41 was characterized by XRD, TEM, nitrogen adsorption analysis, and FT-IR.

3.2.4 Characterization of rice husk silica and RH-MCM-41

Powder XRD patterns were obtained using Cu Kα radiation (1.542 Å) on a Bruker axs D5005 diffractometer. The x-ray was generated with a current of 35 mA and a potential of 35 kV. The samples were scanned from 1 to 15 degrees (2θ) with an increment 0.02 and scan speed 0.5 s/step. The d spacing (d), unit cell size (a) and wall thickness were calculated from the following equations: $d = \dfrac{n\lambda}{2\sin\theta}$,

$a = \dfrac{2}{\sqrt{3}}d$ and wall thickness = a - pore size from N_2 adsorption analysis (Russo et al., 2007).

XRF (EDS Oxford Instrument ED 2000) was used to determine the elemental composition of samples. The samples are prepared for the measurement by borate-fusion technique. One gram of sample was mixed with 7.00 g of flux $Li_2B_4O_7$ in a platinum crucible. Then 0.03 g of LiBr was added to the sample mixture and the platinum crucible was transferred to the fusion machine for melting. After cooling, solidification and casting, the flat lower surface of the disk can be used for XRF analysis in the tube with high voltage and current tube of 40 kV and 30 mA, respectively. Each sample was measured using standard procedure. The measurement time was about 5 min per sample.

N_2 adsorption-desorption isotherm of samples were determined at -196 °C at relative pressure from 0.01 to 0.99 on a Micromeritics (ASAP 2010) analyzer. Before measurement, each sample was degassed and heated at 250 °C for 3 h. The BET surface area was obtained from the N_2 adsorption data in the relative pressure from 0.01 to 0.3. The pore size and pore volumes are calculated from the desorption branches of the isotherm using Barrett-Joyner-Halenda (BJH) method.

The arrangement of mesopores was investigated with a TEM (JEOL JEM 2010). Samples for TEM studies were dispersed in ethanol, dropped on a copper only carbon grid and dried at room temperature with UV light. The voltage for electron acceleration was 120 kV.

Infrared spectra in the mid IR range were obtained from a Perkin-Elmer GX FTIR spectrophotometer with the KBr pellet technique. The solid sample and KBr

were died at 120 °C for 1 h before the measurement. Then 0.5 mg of sample was mixed thoroughly with 30 mg of KBr, ground with an agate mortar and pestle until homogeneous, transferred into sample barrel and pressed with 13 tons force for 1 minute and put on a V-mount cell. The FTIR spectrum was recorded in the range of 400-4000 cm^{-1}.

The as-synthesized RH-MCM-41 was analyzed by TGA on a SDT 2960 thermal analysis system to confirm the template removal. The sample was loaded on an alumina pan, purged with air with a flow rate of 80 mL/min for 1 h and heated from room temperature to 800 °C at a heating rate 10 °C/min.

3.3 Results and discussion

The XRD pattern of rice husk silica was shown in Figure 3.1. Only a broad peak at 22° was observed indicating that the phase of rice husk silica was amorphous. This phase was suitable for the preparation of sodium silicate ($NaSiO_3$) for the synthesis of RH-MCM-41 because it could be easily dissolved in a solution of NaOH. There was a report about a synthesis of ZSM-5 zeolite that used silica from rice husk ash which was calcined at 700 °C. Because silica was in crystalline phase, when it was used for the synthesis of ZSM-5 zeolite, it required a long synthesis time possibly due to the slow dissolution (Kordatos et al., 2008).
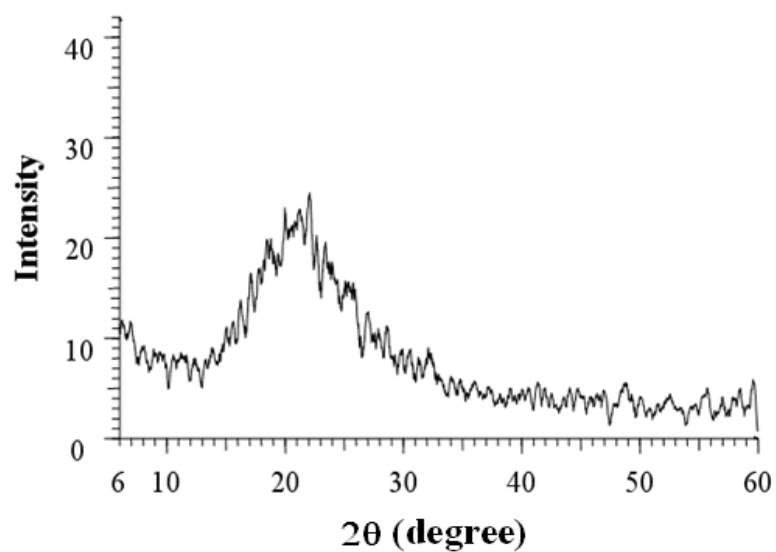
Figure 3.1 XRD spectrum of rice husk silica.

The compositions of rice husk silica determined by XRF are listed in Table 3.1. The purity of rice husk silica was 97.96%, higher than the silica obtained from rice husk ash which was 90% (Yalçin and Sevinç, 2002). The phase and purity of rice husk silica from this method was suitable to use as a silica source for the synthesis of RH-MCM-41.

Table 3.1 Composition of rice husk silica obtain from XRF analysis.

Composition	Concentration (wt%)
SiO_2	97.96
Al_2O_3	0.56
K_2O	0.06
CaO	0.98
Fe_2O_3	0.02

The XRD spectrum of the as-synthesized and the after-calcined RH-MCM-41 are displayed in Figure 3.2. Both samples showed a similar pattern. The strong peak at 2.3° and small peaks at 4.0°, and 4.5° corresponded to the 100, 110 and 200 planes of a hexagonal lattice, respectively (Jing et al., 2002; Park et al., 2002). The d spacing of the 100 planes calculated from Bragg equation was 38.4 Å, similar to the reported value of MCM-41 synthesized with the same template (Jing et al., 2002; Park et al., 2002).

The compositions of RH-MAM-41 are showed in Table 3.2. The major component was silica and there were some amount of alumina and sodium oxide. Alumina was originally found in the rice husk silica and the sodium oxide was transformed from NaOH.

Table 3.2 Composition of RH-MCM-41.

Composition	Concentration(wt%)
SiO_2	97.27
Al_2O_3	0.68
Na_2O	2.04

The N_2 adsorption-desorption isotherm of RH-MCM-41 is shown in Figure 3.3. The isotherm was type IV, typical for mesoporous materials. At the beginning, the adsorbed amount increased quickly and concaved to the P/P_0 axis due to adsorption on external surface to form monolayer. The N_2 adsorption increased from relative pressure of 0.2 again before reaching nearly constant volume at relative pressure of 0.3. This range corresponded to nitrogen adsorption in the mesopores of RH-MCM-41. The adsorbed volume was nearly constant in the rest of the isotherm until an increase again from surface saturation at the relative pressure about 0.9.
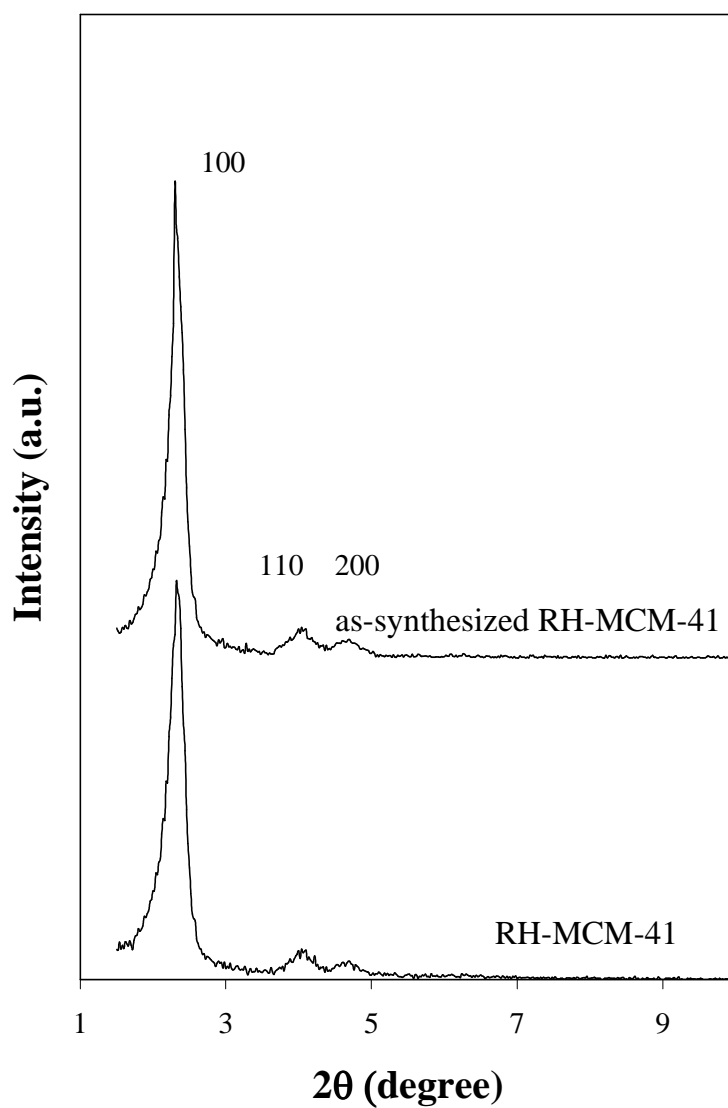
Figure 3.2 XRD spectrum of as-synthesized and calcined RH-MCM-41.
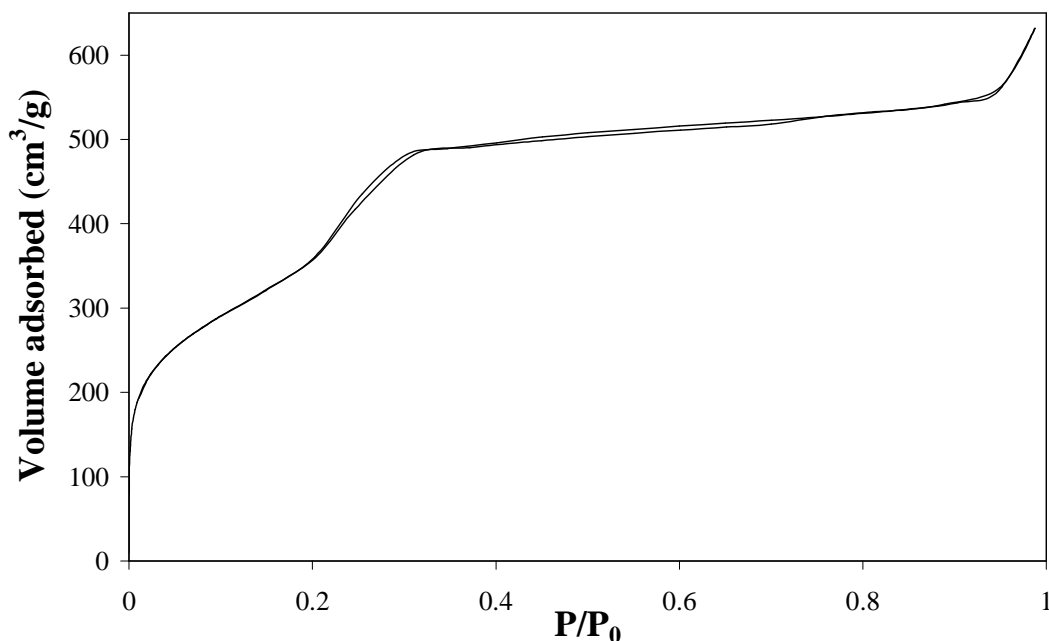
Figure 3.3 N_2 adsorption-desorption isotherm of RH-MCM-41.

Figure 3.4 shows pore size distribution of RH-MCM-41 with the maximum at 29.2 Å which confirmed its mesoporous characteristic. This pore size was similar the reported value of MCM-41 synthesized with the same template which was 30 Å (Jing et al., 2002; Park et al., 2002). The wall thickness of RH-MCM-41 synthesized with rice husk silica by hydrothermal was 16.4 Å, thicker than RH-MCM-41 synthesized with ambient conditions which was 10.5 Å (Chiarakorn et al., 2007). The thicker walls indicated that the RH-MCM-41 synthesized with hydrothermal method was more stable than that synthesized at ambient conditions. Table 3.3 summarizes all physical parameters of RH-MCM-41 from this work.
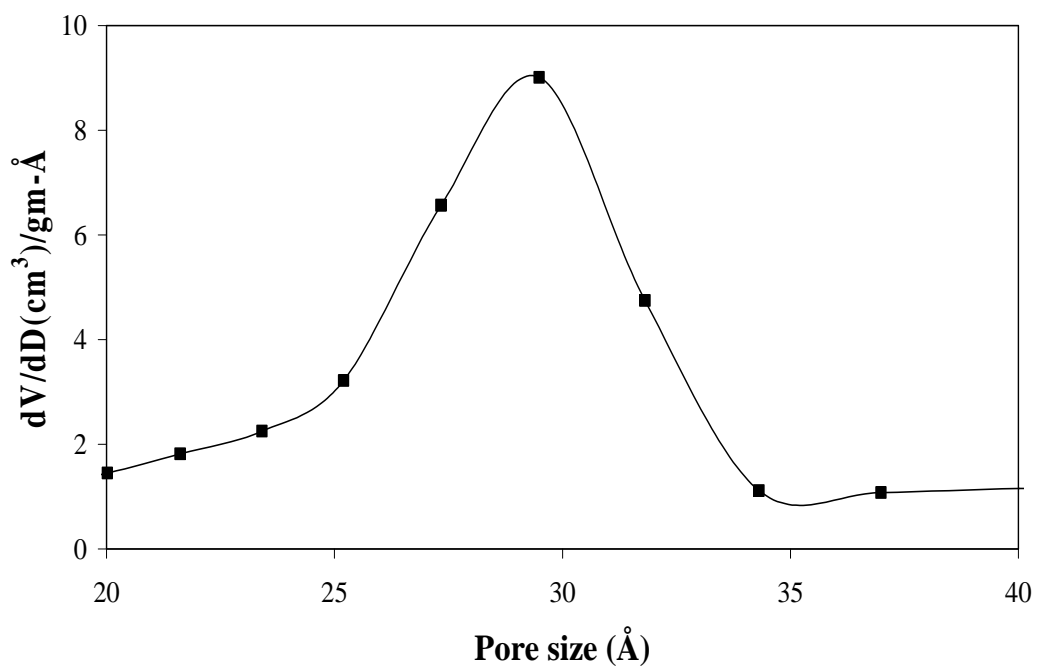
Figure 3.4 Pore size distribution of RH-MCM-41.

Table 3.3 Pore size, wall thickness and surface area of RH-MCM-41.

Sample	d_{100} (Å)	a_{100} (Å)	Pore size (Å)	Wall thickness (Å)	Surface area (m^2/g)
RH-MCM-41[a]	38.4	44.3	29.2	15.1	1335
RH-MCM-41[b]	35.2	40.5	29.0	11.5	800

[a] Hydrothermal method (This work)

[b] Ambient conditions (Chiarakorn et al., 2007)

The TEM micrograph of RH-MCM-41 at magnification of 40k in the Figure 3.5 (left) show non-uniformity of particle size and shape. The right figure taken at higher magnification confirmed an ordered structure characteristic of a regular hexagonal array with the pore size ~ 26 Å.
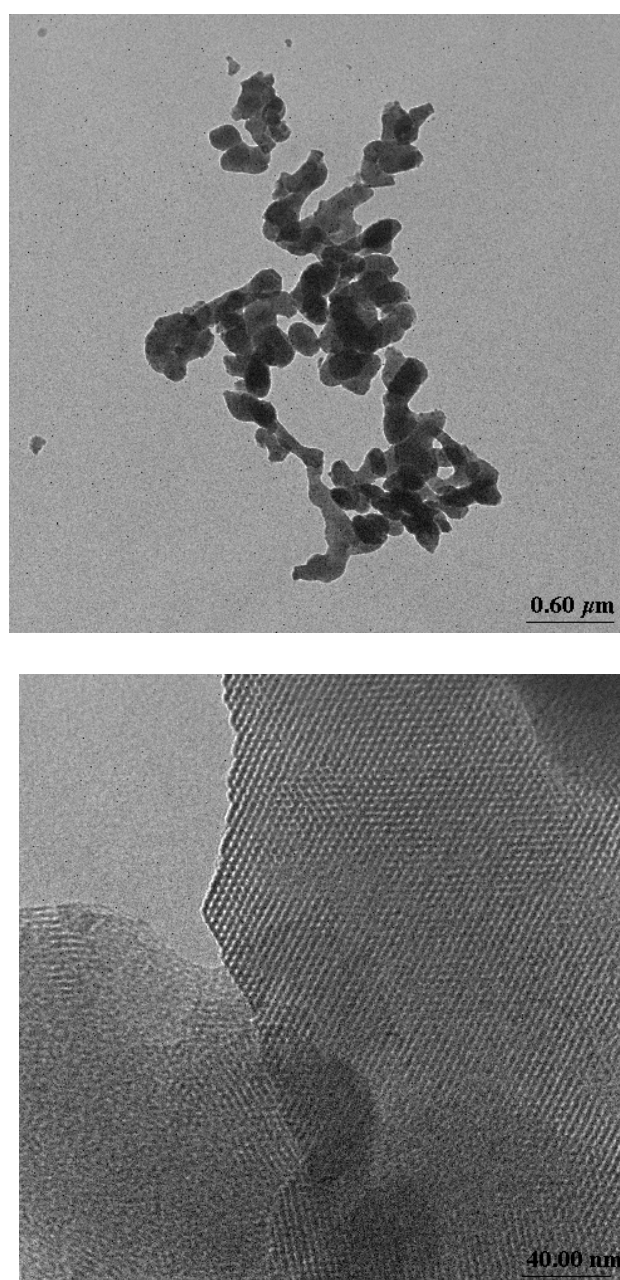
Figure 3.5 TEM micrographs of RH-MCM-41.

The FT-IR spectrum of RH-MCM-41 is shown in Figure 3.6. The presence of absorption bands at 1090, 960, 801 and 461 cm^{-1} corresponded to the Si-O-Si asymmetric stretching, Si-O stretching, Si-O-Si symmetric stretching and Si-O twisting, respectively. The absorption band at 3650 and 1637 cm^{-1} corresponded to -OH stretching of adsorbed water and $-OH_2$ bending mode, respectively, correlated with the water adsorption (hydrophilic property) (Jermy and Pandurangan, 2005).
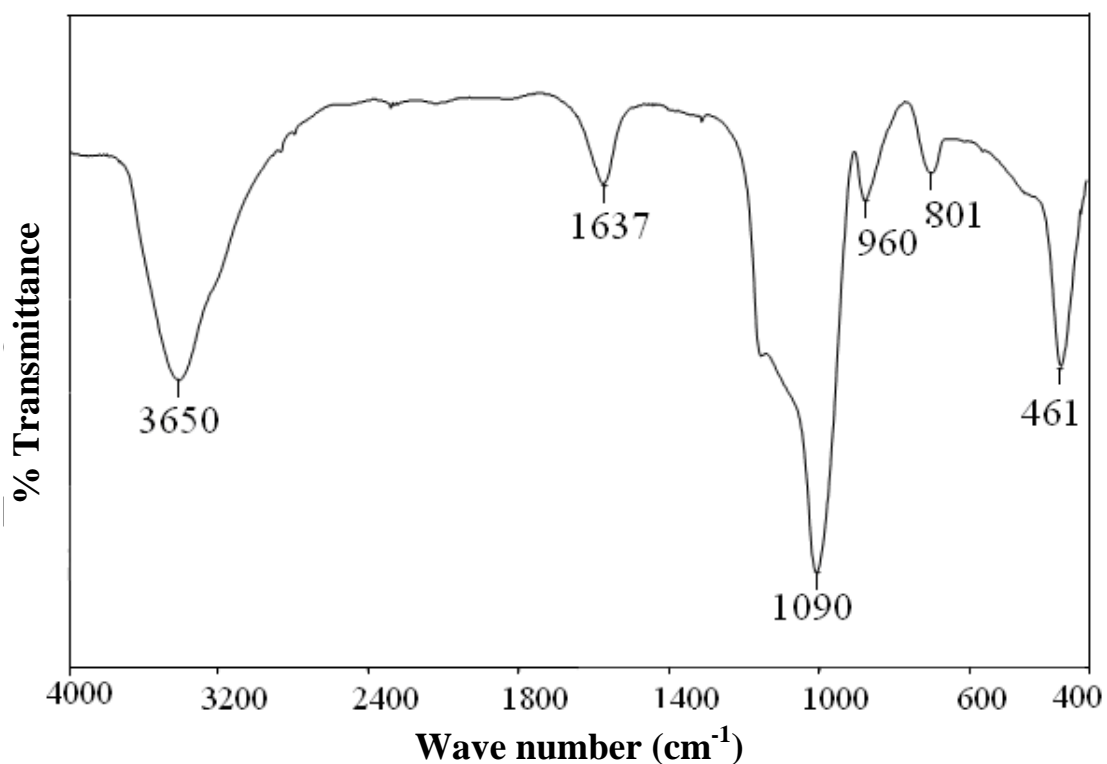
Figure 3.6 FT-IR spectrum of RH-MCM-41.

The thermal property of the as-synthesized RH-MCM-41 was investigated by TGA and the results are shown Figure 3.7. The initial weight loss up to 120 °C was caused by desorption of physically adsorbed water. The weight loss from 120 to 350 °C was assigned to the decomposition of organic template to gaseous products. The weight loss above 350 °C is related to water loss from the condensation of adjacent Si-OH groups to form siloxane bonds (Jermy and Pandurangan, 2005).
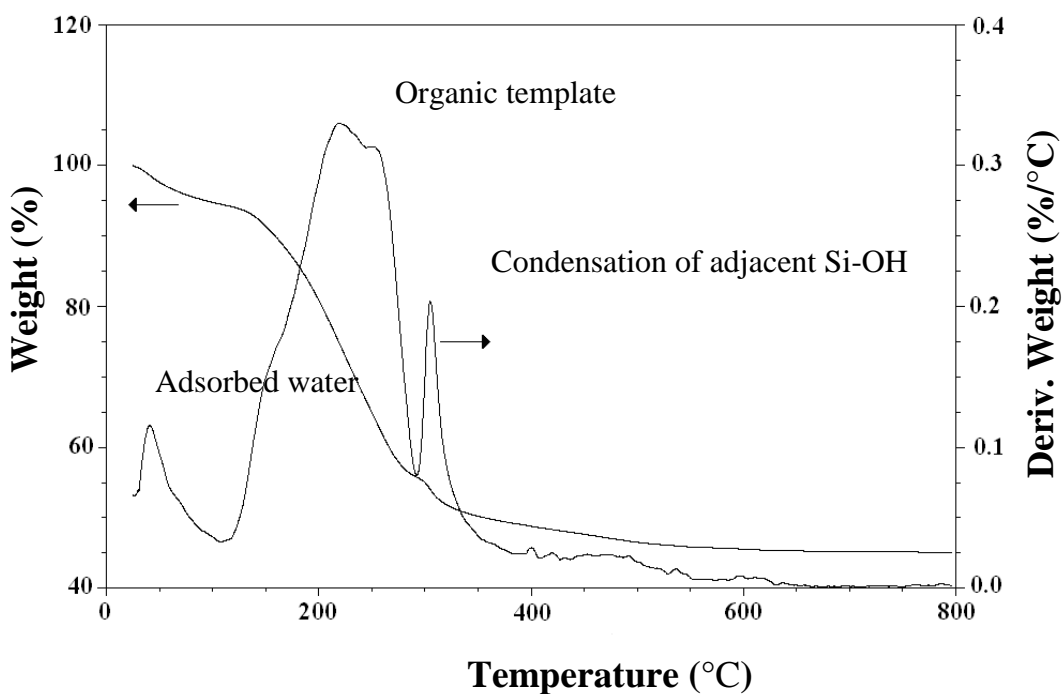
Figure 3.7 TGA result of as-synthesized RH-MCM-41.

3.4 Conclusions

Rice husk silica prepared by acid leaching was in amorphous phase and had purity of 98 wt%. It was suitable to use as a silica source for the synthesis of RH-MCM-41. The synthesis of RH-MCM-41 by hydrothermal method was successful and the structure of the product was confirmed by XRD. The surface area was 1335 m^2/g and the average pore size was 29.2 Å. The RH-MCM-41 synthesized in this work was more stable than that synthesized at ambient conditions which had thinner pore walls. The RH-MCM-41 was also well characterized by TEM, FTIR and TGA.

3.5 References

Chiarakorn, S., Areerob, T. and Grisdanurak, N. (2007). Influence of functional silanes on hydrophobicity of MCM-41 synthesized from rice husk. **Science and Technology of Advanced Materials** 8: 110-115.

Choi, J., Yoon, S., Jang, S. and Ahn, W. (2006). Phenol hydroxylation using Fe-MCM-41 catalysts. **Catalysis Today** 111: 280-287.

Grisdanurak, N., Chiarakorn, S. and Wittayakun, J. (2003). Utilization of mesoporous molecular sieve synthesized from natural source rice husk silica to chlorinated volatile organic compounds (CVOCS) adsorption. **Korean Journal of Chemical Engineering** 20: 950-955.

Huang, S., Jing S., Wang, J., Wang, Z. and Jin, Y. (2001). Silica white obtained from rice husk in fluidized bed. **Powder Technology** 117: 232-238.

Jermy, R. B. and Pandurangan, A. (2005). Catalytic application of Al-MCM-41 in the esterification of acetic acid with various alcohols. **Applied Catalysis A: General** 288 : 25-33.

Jing, H., Guo, Z., Ma, H., Evans, G. D. and Duan, X. (2002). Enhancing the selectivity of benzene hydroxylation by tailoring the chemical affinity of the MCM-41 catalyst surface for the reactive molecules. **Journal of Catalysis** 212: 22-32.

Matsumoto, A., Chen H., Tsutsumi, K., Grün, M. and Unger, K. (1999). Novel route in the synthesis of MCM-41 containing framework aluminum and its characterization. **Microporous Mesoporous Materials** 32: 55-62.

Ming-Tseh, T., and Feg-Wen, C. (2000). Characterization of rice husk ash-supported nickel catalysts prepared by ion exchange. **Applied Catalysis A** 203: 15-22.

Park, K.-C., Yim, D. and Ihm, S (2002) Characteristics of Al-MCM-41 supported Pt catalysts: effect of Al distribution in Al-MCM-41 on its catalytic activity in naphthalene hydrogenation. **Catalysis Today** 74: 281-290.

Krishnarao, R. V., Subrahmanyam, J. and Jagadish Kumar T. (2001). Studies on the formation of black particles in rice husk silica ash. **Journal of the European Ceramic Society** 21: 99-104.

Kordatos, K., Gavela, S., Ntziouni, A., Pistiolas, K. N., Kyritsi, A., and Kasselouri-Rigopoulou, V. (2008). Synthesis of highly siliceous ZSM-5 zeolite using silica from rice husk ash. **Microporous and Mesoporous Materials** 115: 189-196.

Russo, A. P., Carrott, R. L. M. M., Carrott, P. J. M. (2007). Effect of hydrothermal treatment on the structure, stability and acidity of Al containing MCM-41 and MCM-48 synthesised at room temperature. **Colloids and Surfaces A: Physicochemical and Engineering Aspects** 301: 9-19.

Sun, L., and Gong, K. (2001), Silicon-Based Material from rice husks and their applications. **Industrial Engineering Chemistry Research** 40: 5861-5877.

Wittayakun, J., Khemthong, P., and Prayoonpokrach, S. (2008). Synthesis and characterization of zeolite Y from rice husk silica. **Korean Journal of Chemical Engineering** 25: 861-864.

Yalçin, N. and Sevinç, V. (2001). Studies on silica obtained from rice husk. **Ceramics International** 27: 219-224.

CHAPTER IV

CHARACTERIZATION OF PLATINUM-IRON CATALYSTS SUPPORTED ON RH-MCM-41 AND THEIR PERFORMANCES FOR PHENOL HYDROXYLATION

Abstract

The goal of this chapter was to use mesoporous material RH-MCM-41 synthesized with rice husk silica by hydrothermal method as a support for bimetallic platinum-iron catalyst, denoted as Fe-Pt/RH-MCM-41; monometallic Pt/RH-MCM-41 and Fe/RH-MCM-41 catalysts. The catalysts were prepared by co-impregnation with Pt and Fe amount of 0.5 and 5.0% by weight, respectively, and tested for phenol hydroxylation. The RH-MCM-41 structures in all catalysts were confirmed by X-ray diffraction (XRD) and their surface areas were determined by nitrogen adsorption. The oxidation state of Fe supported on RH-MCM-41, analyzed by X-ray absorption near edge structure (XANES) was +3. The transmission electron microscopy (TEM) micrographs of all catalysts displayed well-ordered structure of RH-MCM-41 and nanoparticles of metal could be observed in some catalysts. All catalysts were active for phenol hydroxylation using H_2O_2 as an oxidant when the phenol:H_2O_2 ratios were varied at 2:1, 2:2, 2:3 and 2:4. The first three ratios produced only catechol and hydroquinone whereas the 2:4 ratio produced catechol, hydroquinone and benzoquinone. The 2:3 ratio gave the highest phenol conversion of 47% at 70 °C.

The catalyst prepared by co-impregnation from Pt and Fe precursors was more active than a physical mixture of Pt/RH-MCM-41 and Fe/RH-MCM-41.

4.1. Introduction

This work focused on the utilization of RH-MCM-41 synthesized with rice husk silica by hydrothermal method as a support for bimetallic platinum-iron catalysts, denoted as Pt-Fe/RH-MCM-41. The support with high surface area was expected to provide high metal dispersion and consequently enhance the catalytic performance. The catalysts were characterized by several methods including X-ray diffraction (XRD), transmission electron microscopy (TEM) and X-ray absorption near edge structure (XANES). The surface areas of RH-MCM-41 and bimetallic catalysts were determined by N_2 adsorption-desorption.

The Pt-Fe/RH-MCM-41catalysts were tested for phenol hydroxylation which was a reaction between phenol and H_2O_2 to produce catechol and hydroquinone (see Figure 2.1 in Chapter II). These products are useful chemicals in several applications such as photographic chemicals, antioxidants, flavoring agents, polymerization inhibitors and pharmaceuticals (Matsumoto et al., 1999). This reaction is simple and can be carried out in a batch reactor. In addition, benzoquinone could be produced by further oxidation as a by-product.

The phenol oxidation on Pt catalysts supported on graphite in a stirred tank reactor was studied and the selectivity of the oxidation products depended on the degree of oxygen coverage on platinum surface (Masende et al., 2006). The over-

oxidised platinum was proposed to be favorable for the formation of hydroquinone whereas the partially oxidized platinum was proposed to be favorable for the formation of catechol. The phenol hydroxylation on Fe catalysts was also reported for various supports, temperature and phenol:H_2O_2 ratios (Choi et al., 2006; Wu et al., 2008; Preethi et al., 2008; Liu et al., 2008; Hao et al., 2001; Letaïëf et al., 2008; Mohamed et al., 1993; Abbo et al., 2005) The highest conversion reported, 60% was obtained on Fe/MCM-41 with ~10 wt% Fe at 70 °C with the phenol:H_2O_2 ratio of 1:1 (Choi et al., 2006). The reaction mechanism with H_2O_2 solution over Fe/MCM-41 was proposed that the Fe^{3+} reacted with H_2O_2 to form OH radicals which reacted with phenol to form catechol and hydroquinone (Choi et al., 2006). In addition, the phenol conversion of 58.5% was obtained from Fe/Al-MCM-41 catalyst with 10 wt% Fe at 40 °C (Preethi et al., 2008). The XRD patterns of MCM-41 and Al-MCM-41 showed a decrease of intensity with high amount of Fe added. In the works above, the ratio of starting reagents was only fixed at 1:1. It was interesting to vary the amount of H_2O_2 and to modify Fe catalyst with Pt to increase the product yields.

This work focused on bimetallic Pt-Fe catalysts dispersing on RH-MCM-41. The ratios of phenol/H_2O_2 were varied and the catalytic performance of the bimetallic Pt-Fe/RH-MCM-41 catalyst was compared with monometallic catalysts as well as a physical mixture between Pt/RH-MCM-41 and Fe/RH-MCM-41.

4.2 Experimental

4.2.1 Chemicals

RH-MCM-41 was synthesized by chemicals and method reported in Chapter III. The chemicals for catalyst preparation were iron(III) chloride hexahydrate ($FeCl_3 \cdot 6H_2O$) supplied by Polskie Odczynniki Chemiczne (POCh) and dihydrogen hexachlorplatinate(IV) (40% $H_2PtCl_6 \cdot 6H_2O$) supplied by Alfa.

The chemicals for catalyst testing were phenol (C_6H_5OH) supplied by BDH and hydrogenperoxide (30%, H_2O_2) supplied by Ajax. Standards for product quantitative analysis were cetechol ($C_6H_6O_2$) supplied by Fluka and hydroquinone ($C_6H_4(OH)_2$) supplied by Asia Pacific Speciality Chemicals (APS).

4.2.2 Catalyst preparation

A solution containing $FeCl_3$ and $H_2PtCl_6 \cdot 6H_2O$ with a sufficient concentration to produce Pt/Fe catalyst with Pt and Fe amount of 0.5 and 5 wt% was impregnated to the RH-MCM-41 support. After being dried at 100 °C overnight and calcined at 300 °C for 2 h, the catalyst referred to as 5Fe0.5Pt/RH-MCM-41 was obtained. In addition, other catalysts were prepared with a similar procedure for comparison including 5Fe/RH-MCM-41, 0.5Pt/RH-MCM-41 and a physical mixture of 0.5Pt/RH-MCM-41 and 5Fe/RH-MCM-41. The physically mixed catalyst was prepared by mixing 0.05 g of 5Fe/RH-MCM-41 and 0.05 g of 0.5Pt/RH-MCM-41 and grinding for 30 min to produce 0.1 g catalyst for the catalytic testing.

4.2.3 Catalyst characterization

Powder XRD patterns were obtained using Cu Kα radiation (1.542 Å) on a Bruker axs D5005 diffractometer. The X-ray was generated with a current of 35 mA and a potential of 35 kV. The samples were scanned from 1 to 15 degrees (2θ), increment 0.02 and scan speed 0.5 s/step.

The X-ray absorption spectra in both EXAFS and XANES regions were acquired at beamline 8 of the the Synchrotron Light Research Institute (Public Organization). The X-ray beam was emitted by a storage ring running at 1.2 GeV with a current of 80-250 mA. The Fe K-edge spectra were recorded at room temperature in the transmission mode and X-rays were detected by two ion chambers, the first chamber for incident beam (I_0) was filled with N_2 and the second chamber for transmitted beam (I_1) was filled with Ar/N_2. The spectra were processed conventionally with ATHENA program. A linear background, determined by a least squares fitting of the pro-edge experimental points, was subtracted from the experimental spectrum. The maximum of the first peak of an iron metal foil was then used as the energy reference. The resulting experimental data in the EXAFS region were analyzed by EXAFSPAK program.

N_2 adsorption-desorption isotherm of samples were determined at -196 °C for relative pressure from 0.01 to 0.99 on a Micromeritics (ASAP 2010) analyzer. Before measurement, each sample was degassed and heated at 250 °C for 3 h. The BET surface area was obtained from the N_2 adsorption data in the relative pressure range of 0.01 to 0.3. The pore size and pore volumes are calculated from the desorption branches of the isotherm using Barrett-Joyner-Halenda (BJH) method.

The arrangement of mesopores was investigated with a TEM (JEOL JEM 2010). Samples for TEM studies were dispersed in ethanol, dropped on a copper only carbon grid and dried at room temperature with UV light. The voltage for electron acceleration was 120 kV.

A UV-vis diffuse reflectance spectrum in the range of 220-800 nm was obtained from a HITACHI (UV-3501) spectrometer using $BaSO_4$ as a reference in ambient conditions.

4.2.4 Catalytic testing on phenol hydroxylation

The appatus setup for reaction testing is shown in Scheme 4.1. The 5Fe0.5Pt/RH-MCM-41 catalyst (0.05 g), phenol and H_2O_2 solution (30% w/v) were mixed in a round bottle equipped with a magnetic stirrer and a reflux condenser. The phenol:H_2O_2 mole ratios were 2:1, 2:2, 2:3 and 2:4 and the reaction was carried out at 70 °C for 3 h. Sampling was done every hour and the solution was separated from the catalyst and analyzed by a gas chromatograph (Shimadzu GC14-A) equipped with a capillary column and a flame ionization detector. The GC injector and column temperatures were 220 °C and 190 °C, respectively. The most suitable reactant ratio was further used to test physical mixture of 0.5Pt/RH-MCM-41 and 5Fe/RH-MCM-41 at similar conditions.
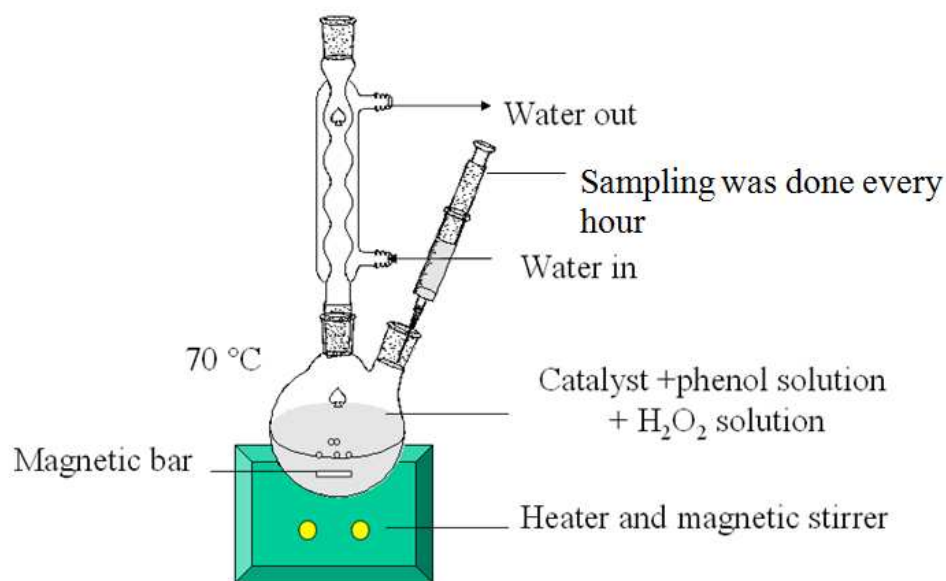
Scheme 4.1 Apparatus set up for catalytic testing.

To confirm the benefit of using mesoporous support, the catalytic performance of the 5Fe0.5Pt/RH-MCM-41 was compared with that of 5Fe0.5Pt/RH-Silica with the most suitable testing conditions as mentioned above.

4.3 Results and discussion

The XRD patterns of the calcined 0.5Pt/RH-MCM-41, 5Fe/RH-MCM-41 and 5Fe0.5Pt/RH-MCM-41 were displayed in Figure 4.1 and 4.2. All catalysts showed characteristic of MCM-41 with a strong peak at 2.5° and small peaks at 4, and 4.5° corresponding to the 100, 110 and 200 planes of a hexagonal lattice, respectively (Jing et al., 2002; Park et al., 2002). The intensity of the main peak decreased after metal addition indicating the decrease of RH-MCM-41 crystallinity. The decrease of the intensity was also caused by blocking of reflection planes of RH-MCM-41 by the metals on the surface. The relative crystallinity of RH-MCM-41 in each catalyst was

calculated by comparing area of the main RH-MCM-41 peak of the catalyst to that of the parent RH-MCM-41. The results are shown in Table 4.1. The peaks of iron and platinum in RH-MCM-41 samples were not detected by XRD indicating that metal particles dispersed well on RH-MCM-41.
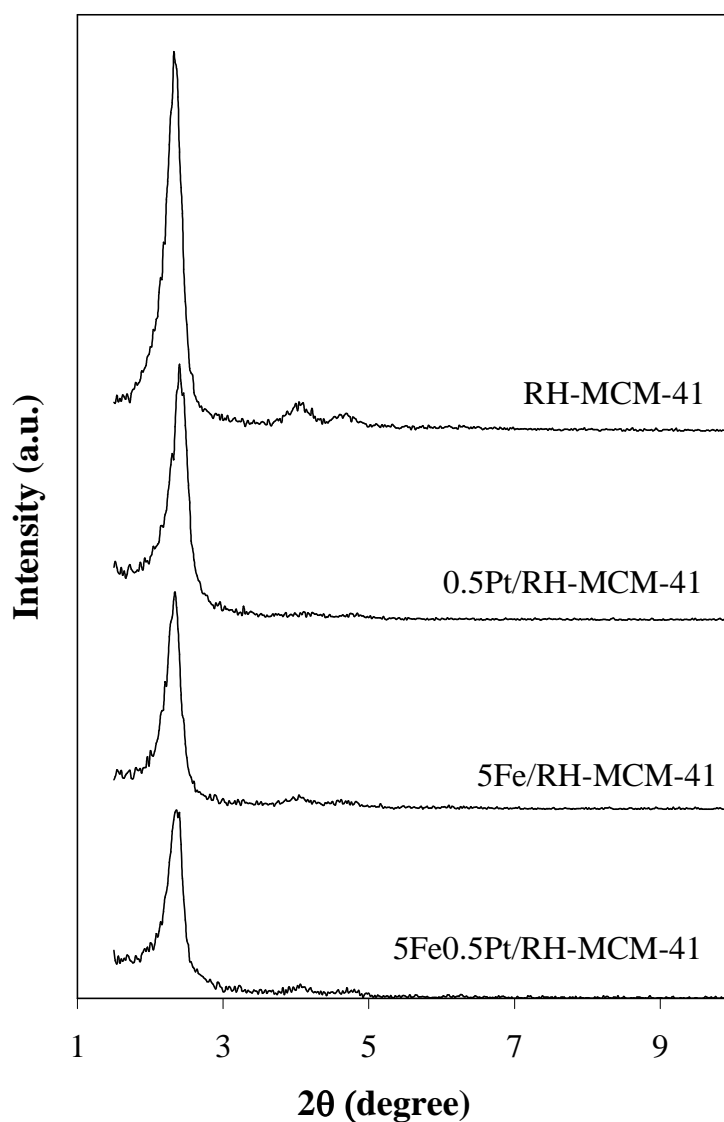
Figure 4.1 XRD patterns of RH-MCM-41 and RH-MCM-41 supported catalysts.
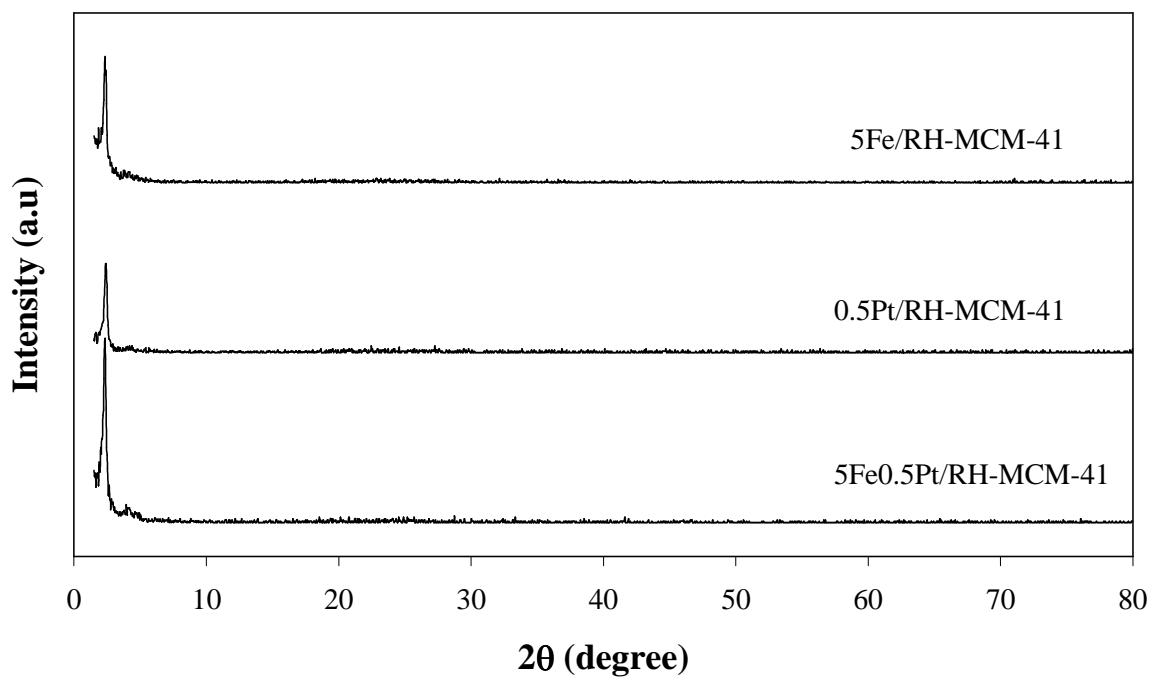
Figure 4.2 XRD patterns of RH-MCM-41 and RH-MCM-41 supported catalysts in
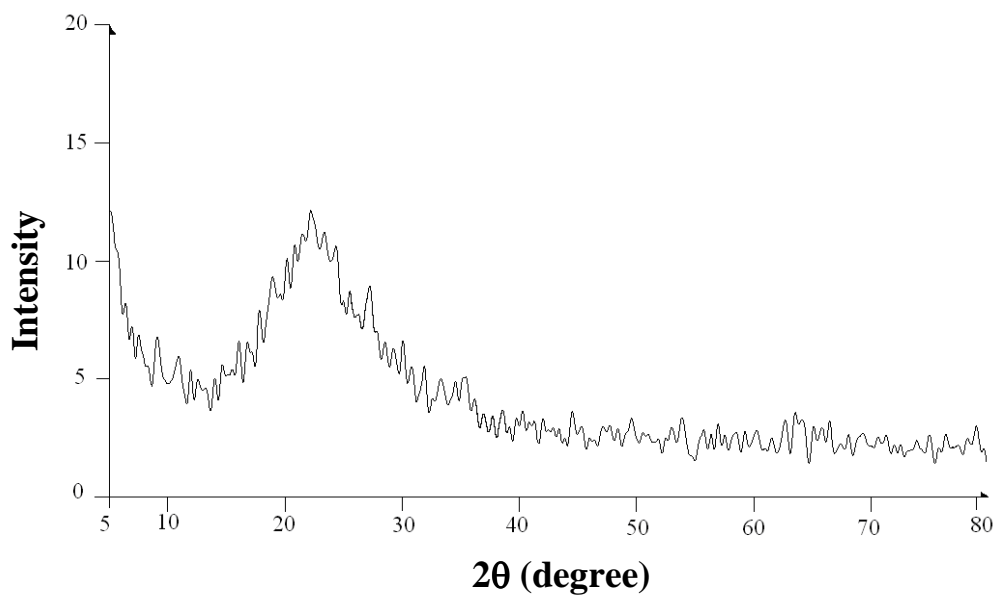
large angles.

Figure 4.3 XRD patterns of silica supported catalysts in large angles.

Table 4.1 Relative crystallinity and surface area of RH-MCM-41 and RH-MCM-41 supported catalysts

Sample	Relative crystallinity (%)	Surface area (m^2/g)	Pore size (Å)
RH-MCM-41	100	1335	29.2
0.5Pt/RH-MCM-41	67	1052	27.9
5Fe0.5Pt/RH-MCM-41	57	964	25.7
5Fe/RH-MCM-41	51	874	25.4

The N_2 adsorption isotherms of 5Fe/RH-MCM-41, 0.5Pt/RH-MCM-41 and 5Fe0.5Pt/RH-MCM-41 are compared with that of parent RH-MCM-41 in Figure 4.4. All isotherms were type IV, typical for mesoporous materials. At the beginning, the adsorbed amount increased quickly and concaved to the P/P_0 axis due to adsorption on external surface to form monolayer. The adsorbed amounts in all catalysts were lower than that of the parent RH-MCM-41 indicating that their surface areas decreased because of the coverage by metal after metal loading. The N_2 adsorption increased again before reaching nearly constant volume in the relative pressure range of 0.2-0.4. This range corresponded to nitrogen adsorption in the mesopores of RH-MCM-41 and catalyst samples. However, the adsorption in this range for the catalysts containing 5 wt% Fe did not increased sharply as in RH-MCM-41 indicating that some mesopores were blocked by metal particles. The pore size distributions are shown in Figure 4.5. The shift to lower size and low peak area indicated that the metal might reside in the pores of RH-MCM-41.
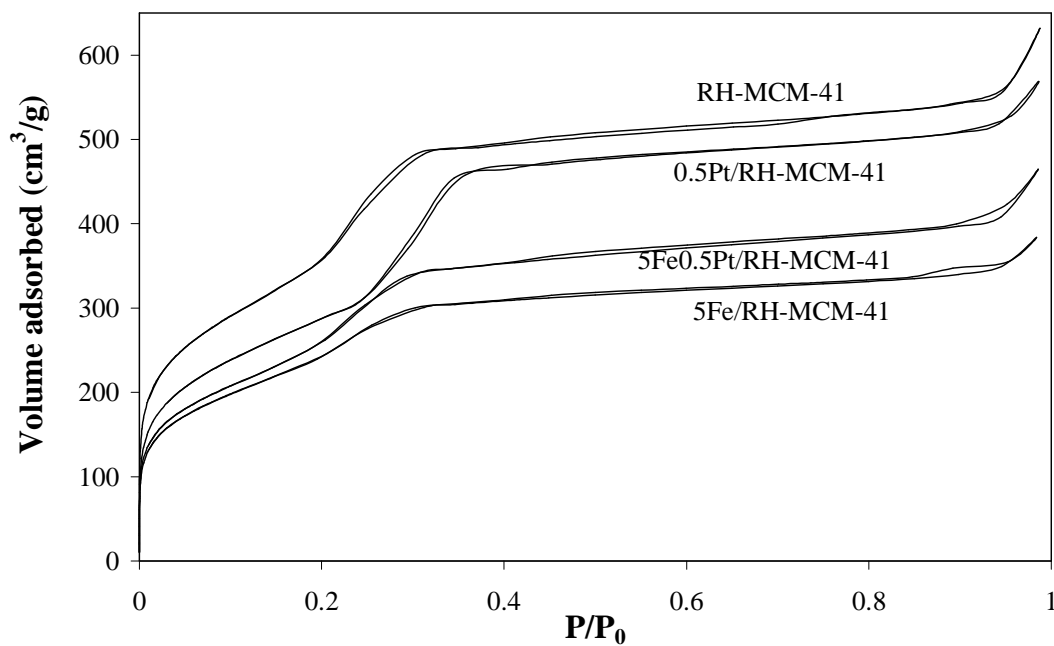
Figure 4.4 N_2 adsorption-desorptiom isotherms of RH-MCM-41 and RH-MCM-41

supported catalysts**.**
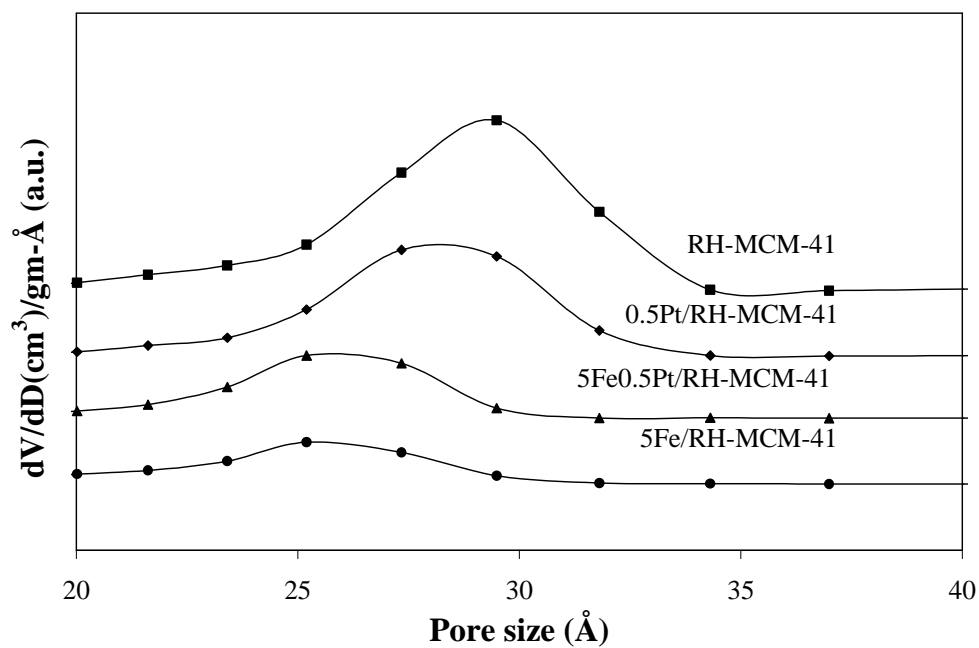
Figure 4.5 Pore size distribution of RH-MCM-41 and RH-MCM-41 supported

catalysts.

The surface area and pore size of RH-MCM-41 and RH-MCM-41 supported catalysts are listed in Table 4.1. Both values decreased after loading RH-MCM-41 with metal.

The TEM micrographs of RH-MCM-41 (Figure 4.6) show ordered structure characteristic of a regular hexagonal array and TEM micrographs of all catalysts displayed well-ordered structure and nanoparticles of metals could be observed in some catalysts.
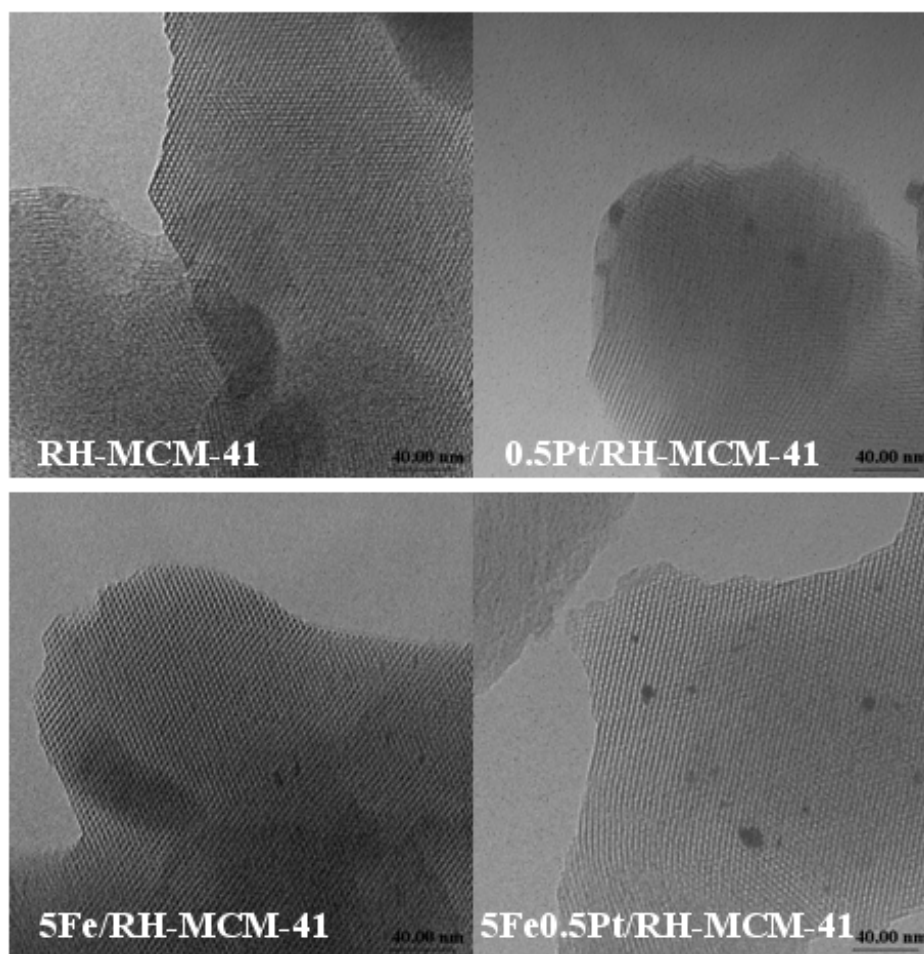
Figure 4.6 TEM micrographs of RH-MCM-41 and RH-MCM-41 supported catalysts.

The Fe K-edge XANES spectra of 5Fe/RH-MCM-41 and 5Fe0.5Pt/RH-MCM-41 were compared to standards compounds containing Fe^0, Fe^{2+} and Fe^{3+} in Figure 4.7 and Table 4.2. The edge position and shape of XANES spectra of Fe in both 5Fe/RH-MCM-41 and 5Fe0.5Pt/RH-MCM-41 were similar to that of the standard Fe^{3+} indicating that the oxidation state of iron in these catalysts was +3.
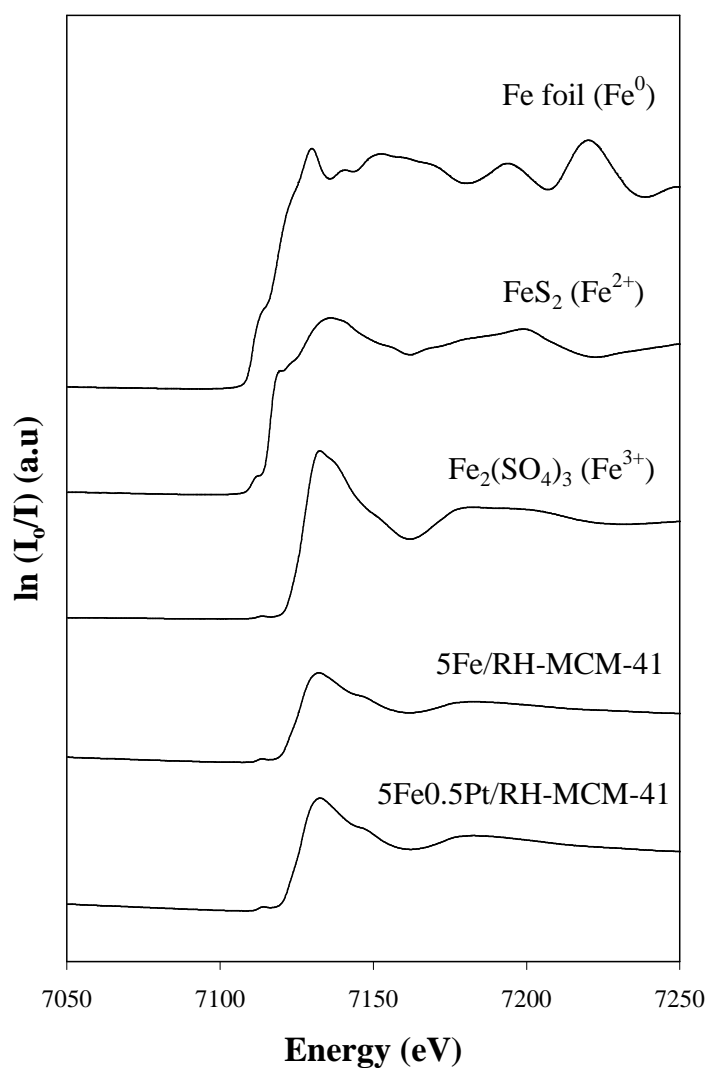
Figure 4.7 Fe K-edge XANES spectra of Fe containing catalysts compared to
reference materials.

Table 4.2 The positions of pre-edge and edge of Fe from XANES spectra.

Sample	Pre-edge (eV)	Edge (eV)
Fe foil (Fe^0)	-	7112
FeS_2 (Fe^{2+})	7111	7116
$Fe_2(SO_4)_3$ (Fe^{3+})	7114	7125
5Fe/RH-MCM-41	7114	7125
5Fe0.5Pt/RH-MCM-41	7114	7125

The Fourier transforms of the k^3-weighted $\chi(k)$ Fe-K EXAFS spectra of 5Fe0.5Pt/RH-MCM-41 is shown in Figure 4.8. The data from fitting show coordination number and radius bond of Fe are shown in Table 4.3. Each Fe atom was surrounded by four oxygen atom in first sell with an average radius (Fe-O) of 1.96 Å. The second shell Fe-Si was also observed. The 5Fe0.5Pt/RH-MCM-41 catalyst showed iron oxide form on the support RH-MCM-41.

Table 4.3 Structural parameters obtained from fitting the Fe K-edge EXAFS data of 5Fe0.5Pt/RH-MCM-41.

Shell	Coordination number	Radius (Å)	$\sigma \times 10^{-2}$	ΔE (eV)
Fe-O	4.9 ±0.2	1.96 ±0.01	1.18 ±0.06	-3.01 ±0.59
Fe-Si	1.6 ±0.2	2.92 ±0.01	0.50 ±0.01	14.88 ±0.27
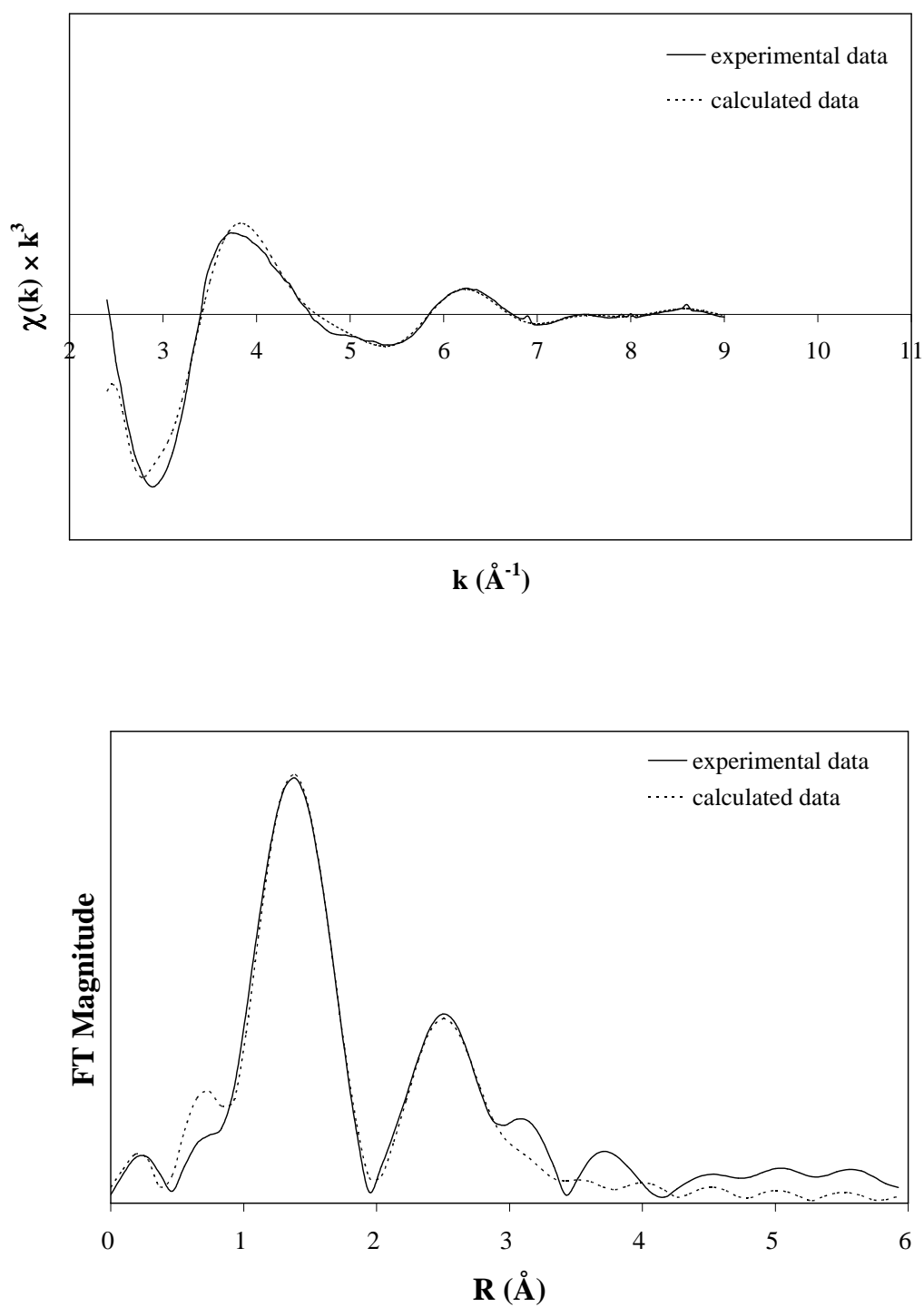
Figure 4.8 (top) EXAFS function (bottom) Fourier transforms of the k^3-weighted $\chi(k)$

Fe-*K* EXAFS spectra of 5Fe0.5Pt/RH-MCM-41.

The UV-vis diffuse reflectance spectra in the wavelength range of 200-800 nm of 5Fe0.5Pt/RH-MCM-41 is shown in Figure 4.7. The dash lines were obtained from taking derivatives of the absorbance. A wide absorption tail was observed in the spectrum indicated indicates the coexistence of various kinds of Fe oxidation states (Choi et al., 2006). A broad band between 220 nm and 250 nm centered at 230 nm, assigned to the low-energy d_π-p_π charge-transfer transitions between tetrahedral oxygen ligands and central Fe^{3+} ion. The tetrahedral environment was typical for framework Fe^{3+} ions in Fe-substituted mesoporous molecular sieves. The bands at 360 and 600 nm were assigned to the Fe species in octahedral coordination Fe_2O_3 crystallites species. This might be due to the formation of nano-crystalloid Fe_2O_3. (Jia et al., 2007; Wu et al., 2008)
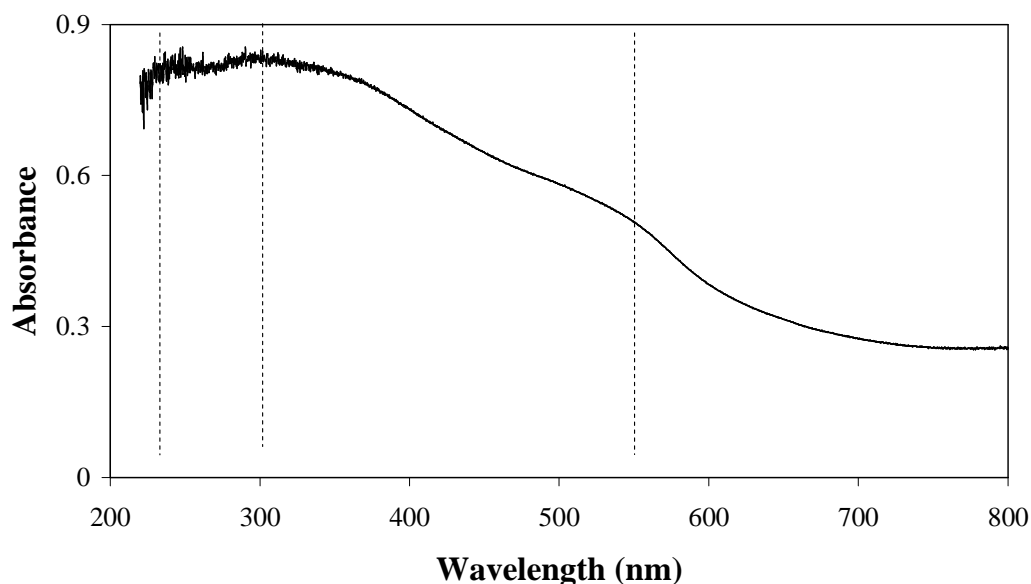
Figure 4.9 UV-vis diffuse reflectance spectra of 5Fe0.5Pt/RH-MCM-41.

Table 4.4 showed the catalytic performance of the 5Fe0.5Pt/RH-MCM-41 catalyst for phenol hydroxylation with phenol:H_2O_2 ratios of 2:1, 2:2, 2:3 and 2:4. The conversion of phenol increased with the amount of H_2O_2. Although the conversion was highest when the phenol:H_2O_2 ratio was 2:4, the selectivity for catechol was lower than other ratios because another product, benzoquinone, from further oxidation was also detected. Because the first three ratios produced only catechol and hydroquinone and the highest conversion among these ratios was obtained when the phenol:H_2O_2 ratio was 2:3. This ratio was considered to be the most suitable for phenol hydroxylation over the 5Fe0.5Pt/RH-MCM-41 catalyst.

The catalytic performance of the 5Fe0.5Pt/RH-MCM-41 was compared with that of the physical mixture of 0.5Pt/RH-MCM-41 and 5Fe/RH-MCM-41 at 70 °C with phenol:H_2O_2 ratio of 2:3. The conversions of phenol are compared in Figure 4.8 and the selectivities are shown in Table 4.5. The bimetallic 5Fe0.5Pt/RH-MCM-41 catalyst prepared by co-impregnation gave a higher conversion of phenol with similar selectivity. This result confirmed that the presence of both Pt and Fe on the same RH-MCM-41 support improved the catalytic performance.

Jia et al. (2007) used a diatomite which contained 0.94% Fe as a catalyst for phenol hydroxylation. The conversion of phenol on the same amount of catalysts (0.5 g) was 40%, similar to this work when the ratio of phenol:H_2O_2 was 1:1 (Jia et al., 2007). However, the diatomite used a longer reaction time and higher temperature (6 h and 80 °C, respectively) than that of the 5Fe0.5Pt/RH-MCM-41. The higher Fe loading in our catalyst and good dispersion on a high surface area RH-MCM-41 might

be the explanation because there were more available active sites for the reaction. The conversion in this work also increased when the phenol:H_2O_2 ratio was increased to 2:3. Choi et al. (2006) proposed reaction mechanism with H_2O_2 solution over Fe/MCM-41 that Fe^{3+} reacted with H_2O_2 to form OH radicals which reacted with phenol to form catechol and hydroquinone. In addition, the side reaction produced O_2 and H^+ and the O_2 could possibly cover on Pt to generate OH radicals for the hydroxylation.

The catalytic performance of the 5Fe0.5Pt/RH-MCM-41 was also compared with that of 0.5Pt5Fe/RH-Silica to confirm the contribution of mesoporous support. Because the surface area of RH-MCM-41 was significantly higher than that of RH-SiO_2 (1335 vs 235 m^2/g), the better metal dispersion a better catalytic performance was expected. The results in Figure 4.10 and Table 4.5 showed that the phenol hydroxylation on 5Fe0.5Pt/RH-Silica occurred more slowly and gave lower conversion of phenol. Thus, the dispersion of Pt-Fe on mesoporous RH-MCM-41 could improve the catalytic performance.

Table 4.4 Catalytic performance of 5Fe0.5Pt/RH-MCM-41 on phenol hydroxylation

at 70 °C with various phenol:H_2O_2 ratios.

Phenol:H_2O_2	Time (h)	% Conversion	% Selectivity		
			Catechol	Hydroquinone	Benzoquinone
2:1	0.5	23.1	51.1	48.9	-
	1	24.9	50.8	49.2	-
	2	25.0	52.2	47.8	-
	3	25.2	52.2	47.8	-
2:2	0.5	41.3	52.6	47.4	-
	1	37.9	52.7	47.4	-
	2	42.9	51.9	48.1	-
	3	38.1	51.8	48.2	-
2:3	0.5	43.6	55.7	44.3	-
	1	47.6	54.4	45.6	-
	2	47.3	54.7	45.3	-
	3	46.6	54.6	45.4	-
2:4	0.5	64.8	43.1	35.9	21.0
	1	62.7	44.9	37.7	17.4
	2	63.1	45.6	38.8	15.7
	3	64.9	42.5	35.8	21.7

Table 4.5 Selectivities for phenol hydroxylation of 5Fe0.5Pt/RH-MCM-41, the physical mixture of 0.5Pt/RH-MCM-41 and 5Fe/RH-MCM-41, and 5Fe0.5Pt/RH-Silica with Phenol:H_2O_2 ratio of 2:3 at 70 °C.

Catalyst	Time (h)	Phenol conversion	% Selectivity	
			Catechol	Hydroquinone
5Fe0.5Pt/RH-MCM-41	0.5	43.57	55.7	44.3
	1	47.57	54.4	45.6
	2	47.3	54.7	45.3
	3	46.64	54.6	45.4
Physical mixture of	0.5	33.38	56.5	43.5
5Fe/RH-MCM-41 and	1	36.38	55.5	44.5
0.5Pt/RH-MCM-41	2	38.83	54.5	45.5
	3	38.94	53.6	46.4
5Fe0.5Pt/RH-Silica	0.5	-	-	-
	1	6.82	100.0	
	2	40.67	57.9	42.1
	3	41.13	57.9	42.1
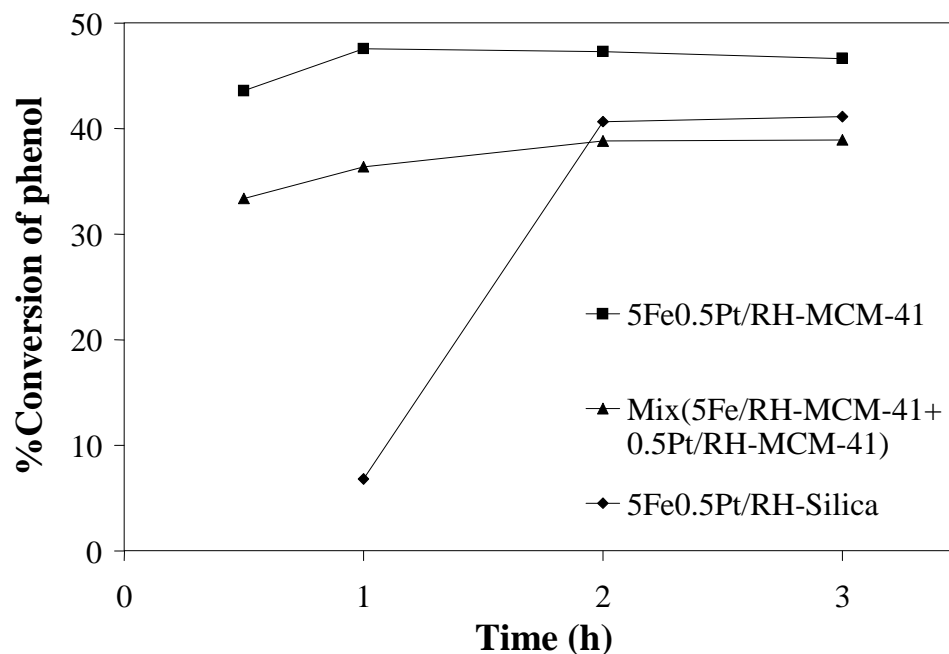
Figure 4.10 Percent conversion of phenol on 5Fe0.5Pt/RH-Silica, 5Fe0.5Pt/RH-

MCM-41 and the physical mixture of 0.5Pt/RH-MCM-41 and 5Fe/RH-

MCM-41.

4.4 Conclusions

When the 5Fe0.5Pt/RH-MCM-41 catalyst was prepared by co-impregnation, the crystallinity and surface area decreased upon metal addition. Metal particles could be observed on RH-MCM-41 and the oxidation state of iron was +3. The catalyst was active for phenol hydroxylation using H_2O_2 oxidant when the phenol:H_2O_2 ratios were varied at 2:1, 2:2, 2:3 and 2:4. The first three ratios produced only catechol and hydroquinone whereas the 2:4 ratio produced benzoquinone, thus, the 2:3 ratio was considered to most suitable one. The catalyst prepared by co-impregnation from Pt and Fe precursors was more active than a physical mixture of 0.5Pt/RH-MCM-41 and 5Fe/RH-MCM-41. The catalytic performance of 5Fe0.5Pt/RH-MCM-41 was better

than that of 0.5Pt5Fe/RH-Silica because the RH-MCM-41 support had a significantly

higher surface area, resulting in a better metal dispersion.

4.5 References

Abbo, H. S., Titinchi, S. J., Prasad, R., and Hand, S. (2005). Synthesis, characterization and study of polymeric iron(III) complexes with bidentate *p*-hydroxy Schiff bases as heterogeneous catalysts. **Journal of Molecular Catalysis A: Chemical** 225: 225-232.

Chiarakorn, S., Areerob, T. and Grisdanurak, N. (2007). Influence of functional silanes on hydrophobicity of MCM-41 synthesized from rice husk. **Science and Technology of Advanced Materials** 8: 110-115.

Choi, J., Yoon, S., Jang, S. and Ahn, W. (2006). Phenol hydroxylation using Fe-MCM-41 catalysts. **Catalysis Today** 111: 280-287.

Grisdanurak, N., Chiarakorn, S. and Wittayakun, J. (2003). Utilization of mesoporous molecular sieve synthesized from natural source rice husk silica to chlorinated volatile organic compounds (CVOCS) adsorption. **Korean Journal of Chemical Engineering** 20: 950-955.

Hao, W., Luo, Y., Deng, P. and Li, Q. (2001). Synthesis of Fe-MCM-48 and its catalytic performance in phenol hydroxylation. **Catalysis Letters** 73: 199-202.

Jia, J., Shen, J., Lin, L., Xu, Z., Zhang, T. and Liang, D. (1999). A study on reduction behaviors of the supported platinum-iron catalysts. **Journal Molecular Catalysis A: Chemical** 138: 177-184.

Jia, Y., Han, W., Xiong, G., and Yang, W. (2007). Diatomite as high performance and environmental friendly catalysts for phenol hydroxylation with H_2O_2. **Science and Technology of Advanced Materials** 8: 106-109.

Jing, H., Guo, Z., Ma, H., Evans, D. G. and Duan, X. (2002). Enhancing the selectivity of benzene hydroxylation by tailoring the chemical affinity of the MCM-41 catalyst surface for the reactive molecules. **Journal of Catalysis** 212: 22-32.

Kannan, S., Dubey, A. and Knozinger, H. (2005). Synthesis and characterization of CuMgAl ternary hydrotalcites as catalysts for the hydroxylation of phenol. **Journal of Catalysis** 231: 381-392.

Letaïef, S., Casal, B., Aranda, P., Martín-Luengo, M. A. and Ruiz-Hitzky, E. (2003). Fe-containing pillared clays as catalysts for phenol hydroxylation. **Applied Clay Science** 22: 263-277.

Liu, H., Lu, G., Guo, Y., Guo, Y. and Wang, J. (2008). Study on the synthesis and the catalytic properties of Fe-HMS materials in the hydroxylation of phenol. **Microporous and Mesoporous Materials** 108: 56-64.

Matsumoto, A., Chen H., Tsutsumi, K., Grün, M. and Unger, K. (1999). Novel route in the synthesis of MCM-41 containing framework aluminum and its characterization. **Microporous Mesoporous Materials** 32: 55-62.

Masende, G. P. Z., Kuster, M. F. B., Ptasinski, J. K., Janssen, G. J. J. F., Katima, Y. H. J. and Schouten C. J. (2003). Platinum catalysed wet oxidation of phenol in a stirred slurry reactor; the role of oxygen and phenol loads on reaction pathways. **Catalysis Today** 79-80: 357-370.

Mohamed, M. M., and Eissa, N. A. (2003). Characterization of intrazeolitic Fe^{3+} prepared by chemical vapor deposition of $[(C_5H_5)Fe(CO)_2]_2$ inside NaY and FSM-16 zeolites and their catalytic activities towards phenol hydroxylation. **Materials Research Bulletin** 38: 1993-2007.

Park, J.-N., Wang, J., Choi, Y. K., Dong, W.-Y., Hong, S.-I., Lee, W. C. (2006). Hydroxylation of phenol with H_2O_2 over Fe^{2+} and/or Co^{2+} ion-exchanged NaY catalyst in the fixed-bed flow reactor. **Journal Molecular Catalysis A: Chemical** 247: 73-79.

Park, K.-C., Yim, D. and Ihm, S (2002). Characteristics of Al-MCM-41 supported Pt catalysts: effect of Al distribution in Al-MCM-41 on its catalytic activity in naphthalene hydrogenation. **Catalysis Today** 74:281-290.

Preethi, M. E. L., Revathi, S., Sivakumar, T., Manikandan, D., Divakar, D., Rupa, A. V., and Palanichami, M. (2008). Phenol hydroxylation using Fe/Al-MCM-41 catalysts. **Catalysis Letters** 120: 56-64.

Wittayakun, J., Khemthong, P., and Prayoonpokrach, S. (2008). Synthesis and characterization of zeolite Y from rice husk silica. **Korean Journal of Chemical Engineering** 25: 861-864.

Wu, C., Kong, Y., Gao, F., Wu, Y., Lu, Y., Wang, J. and Dong, L. (2008). Synthesis, characterization and catalytic performance for phenol hydroxylation of Fe-MCM41 with high iron content. **Microporous and Mesoporous Materials** 113: 163-170.

CHAPTER V

CHARACTERIZATION OF RH-AlMCM-41 SYNTHESIZED WITH RICE HUSK SILICA AND UTILIZATION AS SUPPORTS FOR PLATINUM-IRON CATALYSTS

Abstract

RH-MCM-41 was synthesized by using silica from rice husk and further modified to increase acidity by adding Al with grafting method with Si/Al ratio of 75 and 25. The resulting materials were referred to as RH-AlMCM-41(75) and RH-AlMCM-41(25). The XRD spectra of all RH-AlMCM-41 confirmed a mesoporous structure of MCM-41. Surface areas of all RH-AlMCM-41 were in the range of 700-800 m^2/g, lower than that of the parent RH-MCM-41 which was 1230 m^2/g. After Al addition the Si/Al ratio of RH-AlMCM-41(75) and RH-AlMCM-41(25) were higher than that of the parent RH-MCM-41. The RH-AlMCM-41 materials were used as supports for bimetallic platinum–iron catalysts, denoted as Pt-Fe/RH-AlMCM-41, with Pt and Fe amount of 0.5 and 5.0% by weight, respectively. Results from temperature programmed reduction (TPR) indicated that the presence of Al might assist the interaction between Pt and Fe as the reduction temperature of iron oxides shifted to a lower value. All catalysts were active for phenol hydroxylation using H_2O_2 as an oxidant for which the highest conversions was observed on that on RH-

MCM-41 material that had the highest surface area. The acidity of the supports did not present a significant role in improving the catalytic performance.

5.1 Introduction

This work focused on continuation of using rice husk silica as a source for the synthesis of MCM-41 which was further modified with Al.

Mesoporous MCM-41 is amorphous silica with a regular mesopore system (pore size 2-50 nm) which consists of an array of unidimensional and hexagonally shaped mesopores. MCM-41 has attracted considerable interest as a model substance of gas adsorption and catalyst support (Matsumoto et al., 1999). However, it has relatively low surface acidity and a modification to increase acidity is necessary for the applications of MCM-41 for acid-catalyzed reactions such as cracking, isomerization, alkylation and hydroxylation (Matsumoto et al., 1999; Shylesh et al., 2004; Park et al., 2002). Brønsted acid sites on surface of MCM-41 could be generated through isomorphous substitution of Si by Al. There are two methods to introduce Al to MCM-41: direct sol–gel method (Pre) and post-synthetic grafting method (Post). Modification of MCM-41 by the sol-gel method was reported to have unfavorable hydrothermal structural deterioration and relatively low concentration and strength of Brønsted acid sites even at high aluminum content (Park et al., 2002). Therefore, post-synthesis modifications have been developed to maintain structural stability and to incorporate various metal elements into siliceous MCM-41 support. In this work, MCM-41 synthesized with rice husk silica was modified to increase acidity by adding Al with grafting method with Si/Al ratio of 75 and 25. They will be referred to as

RH-AlMCM-41. The products were characterized by X-ray fluorescence (XRF), X-ray diffraction (XRD), transmission electron microscopy (TEM) and N_2 adsorption-desorption (BET method). They were further used as catalyst supports for palladium and iron which were tested for phenol hydroxylation.

The phenol hydroxylation to produce dihydroxybenzenes is an important selective oxidation reaction in which the products. The 1,2-dihydroxybenzene or catechol and 1,3-dihydroxybenzene or hydroquinone are used in various applications such as photographic chemicals, antioxidants, flavoring agents, polymerization inhibitors and pharmaceuticals (Kannan et al., 2005). The process of phenol hydroxylation with 30% H_2O_2 would be a useful process in the future because of its simplicity and lack of pollution. Redox molecular sieves, which are promising materials for transformations of large organic molecules in liquid phase reactions, had emerged recently by incorporating various transition metal species such as platinum and iron (Kannan et al., 2005; Choi et al., 2006; Kuznetsova et al., 2005; Masende et al., 2006). In this work, the catalysts consisting of bimetallic platinum/iron supported on RH-AlMCM-41 were tested for the hydroxylation of phenol. The percent conversions of phenol at different reaction time were determined.

5.2 Experimental

5.2.1 Chemicals

The chemicals for MCM-41 preparation were cetyltrimethyl ammonium bromide (CTAB), ($C_{16}H_{33}N(CH_3)_3Br$) supplied by Fluka, sodium hydroxide,

anhydrous pellet (NaOH) supplied by Carlo Erba, sulphuric acid 96% (H_2SO_4) supplied by Carlo Erba and sodium aluminate anhydrous ($NaAlO_2$) supplied by Fluka.

The chemicals for catalyst preparation are iron(III)chloride hexahydrate ($FeCl_3 \cdot 6H_2O$) supplied by Polskie Odczynniki Chemiczne (POCh) and dihydrogen hexachlorplatinate(IV) 40% ($H_2PtCl_6 \cdot 6H_2O$) supplied by Alfa.

The chemicals for catalyst testing are phenol (C_6H_5OH) supplied by BDH, hydrogenperoxide 30% (H_2O_2) supplied by Ajax, cetechol ($C_6H_6O_2$) supplied by Fluka and hydroquinone ($C_6H_4(OH)_2$) supplied by Asia Pacific Speciality Chemicals (APS).

5.2.2 Preparation of RH-AlMCM-41

RH-AlMCM-41 supports with Si/Al ratio of 75 and 25 were prepared from the parent RH-MCM-41 and $NaAlO_2$ by grafting method with a procedure from literature (Park et al., 2002). The starting materials 0.5 g were mixed with and aqueous $NaAlO_2$ solution of 25 ml with Si/Al ratio of 75 and 25 in a polypropylene bottle and stirred vigorously for 30 min. Then the solid powder was separated by centrifugation, dried at 100 °C overnight and calcined at 300 °C for 2 h. The RH-AlMCM-41 with Si/Al ratio of 75 and 25 were referred to as RH-AlMCM-41(75) and RH-AlMCM-41(25) throughout this article.

5.2.3 Characterization of RH-AlMCM-41

Powder XRD patterns were obtained using Cu Kα radiation (1.542 Å) on a Bruker axs D5005 diffractometer. The x-ray was generated with a current of 35 mA and a potential of 35 kV. The samples were scanned from 1 to 15 degrees (2θ), increment 0.02 and scan speed 0.5 sec/step.

XRF (EDS Oxford Instrument ED 2000) was used to determine the composition of samples. The samples are prepared for the measurement by Borate-fusion technique. Approximately 1.00 g of sample was mixed with 7.00 g of flux $Li_2B_4O_7$ in the platinum crucible. Then 0.03 g of LiBr was added to the mixture sample and the platinum crucible was transferred to the fusion machine to melt the mixture. After cooling, solidification and casting, the flat lower surface of the disk can be used for XRF analysis in the tube with high voltage and current tube of 40 kV and 30 mA, respectively. Each sample was measured using standard procedure. The measurement time is about 5 min per sample (Buurman et al., 1996).

The acidity of each sample was determined by ammonia adsorption on a TGA, (NETZSCH, model STA 409PC) where the weight changes due to adsorption and desorption were measured directly from a microbalance. Each sample (approximately 100 mg) was pretreated by heating from room temperature to 300 °C in nitrogen flow (flow rate 30 mL/min and heating rate of 10 °C/min) and held for 1 h to remove water. After cooling down to room temperature, the sample was exposed to ammonia in nitrogen (20% and total flow rate 40 mL/min) until the maximum adsorption was obtained. Then it was purged with nitrogen (flow rate 30 mL/min) to remove

physisobred ammonia until the weight became constant. The acidity was calculated from the weight changes and reported as mmol of ammonia per gram of material (mmol/mol).

The arrangement of mesopores was investigated with a TEM (JEOL JEM 2010). Samples for TEM studies were dispersed in ethanol, dropped on a copper only carbon grid and dried at room temperature with UV light. The voltage for electron acceleration was 120 kV.

N_2 adsorption-desorption isotherm of samples were determined at -196 °C for relative pressure from 0.01 to 0.99 on a micromeritics (ASAP 2010) analyzer. Before measurement, each sample was degassed with heat at 250 °C for 3 h. The BET surface area was obtained from the N_2 adsorption data in the relative pressure range of 0.01 to 0.3. The pore size and pore volumes are calculated from the desorption branches of the isotherm using Barrett-Joyner-Halenda (BJH) method.

5.3.4 Preparation of 0.5Pt5Fe/RH-AlMCM-41

The 0.5 wt% of platinum and 5 wt% of iron catalyst supported on RH-AlMCM-41was prepared by co-impregnation with 0.45 M of $FeCl_3$ and 4.8×10^{-3} M of $H_2PtCl_6 \cdot 6H_2O$. The materials were dried at 100 °C overnight and calcined at 300 °C for 2 h, with a heating rate of 10 °C/min. The catalysts obtained were 0.5Pt5Fe/RH-MCM-41, 0.5Pt5Fe/RH-AlMCM-41(75) and 0.5Pt5Fe/RH-AlMCM-41(25).

5.3.5 Characterization of catalysts

In each temperature-programmed reduction (TPR) measurement, a catalyst sample with approximately 50 mg was packed in a quartz tube, pretreated by heating from room temperature to 300 °C in helium flow (flow rate 20 mL/min and ramp rate of 10 °C/min) and held for 1 h to remove water. After cooling down to room temperature, a gas mixture containing 5% H_2 in He was introduced with flow rate of 2 mL/min and the temperature was ramped again with the rate 5 °C/min from room temperature to 600 °C. The water from reduction was detected continuously by a mass spectrometer and plotted with temperature.

A UV-vis diffuse reflectance spectrum was obtained from a HITACHI (UV-3501) spectrometer using $BaSO_4$ as a reference in the range of 220-800 nm in ambient conditions.

5.3.6 Catalytic testing for phenol hydroxylation

The catalytic testing for phenol hydroxylation, the catalyst, phenol and H_2O_2 solution (30% w/v) were mixed (phenol:H_2O_2 mole ratio = 2:3) in a two-necked round bottom flask (250 mL) equipped with a magnetic stirrer and a reflux condenser. The reaction was carried out at 70 °C for 4 h and the catalyst was separated by centrifugation. The product was sampled every hour and analyzed by a gas chromatography (Shimadzu GC14-A) with a capillary column (ID-BP1 3.0 μm, 30 m × 0.53 mm), a flame ionization detector (FID) and the injector and column temperatures were 250 °C and 190 °C, respectively.

5.3 Results and discussion

Because the aluminum was added to RH-MCM-41 by grafting in which the support was mixed with a solution of $NaAlO_2$ and stirred vigorously, some aluminum might remain in the solution. Thus, it was necessary to determine the actual amount of aluminum deposited on RH-MCM-41 by XRF. The obtained Si/Al ratios and calculated acidities of RH-MCM-41 and RH-AlMCM-41 are displayed in Table 5.1. The Si/Al ratios were slightly lower than the calculated values because there was some aluminum presented in the rice husk silica source. The amount of Al added to the parent RH-MCM-41 was significant to change the Si/Al ratio and calculated acidity.

Table 5.1 Si/Al ratio of RH-MCM-41 and RH-AlMCM-41.

Sample	Si/Al ratio from preparation	Si/Al ratio from XRF	Calculated acidity[b] (mmol/g)
RH-MCM-41	-	118.3[a]	0.29
RH-AlMCM-41(75)	75.0	67.7	0.52
RH-AlMCM-41(25)	25.0	23.6	1.4

[a]rice husk silica contained 0.56wt% of Al_2O_3,   [b]based on XRF

Thermograms from ammonia adsorption and desorption of RH-MCM-41 and RH-AlMCM-41 are shown in Figure 5.1. The ammonia adsorption capacity of the calcined samples are listed in the last column of Table 5.2. The capacity increased as the amount of grafted Al was increased. The adsorption capacities from ammonia adsorption was higher than the acidities obtained from XRF for all materials because the adsorption and desorption was carried out at room temperature and the adsorbed amount included both chemisorption and physisorption.

The XRD patterns of the calcined supports and catalysts are displayed in Figure 5.2. All RH-AlMCM-41 had only the main peak of the 100 plane with lower intensity than that of the parent RH-MCM-41 indicating the decrease of crystallinity after Al grafting. The relative crystallinity of each RH-AlMCM-41 compared to the parent RH-MCM-41 was calculated from area of the main peak. The results are shown in Table 5.3. After grafting aluminium could in principle be found as isolated atoms or as aggregates of alumina. The peaks of alumina in RH-AlMCM-41(75) and RH-AlMCM-41(25) samples were not detected by XRD (see Figure 5.3) indicating that aluminum was well dispersed on the MCM-41 framework.
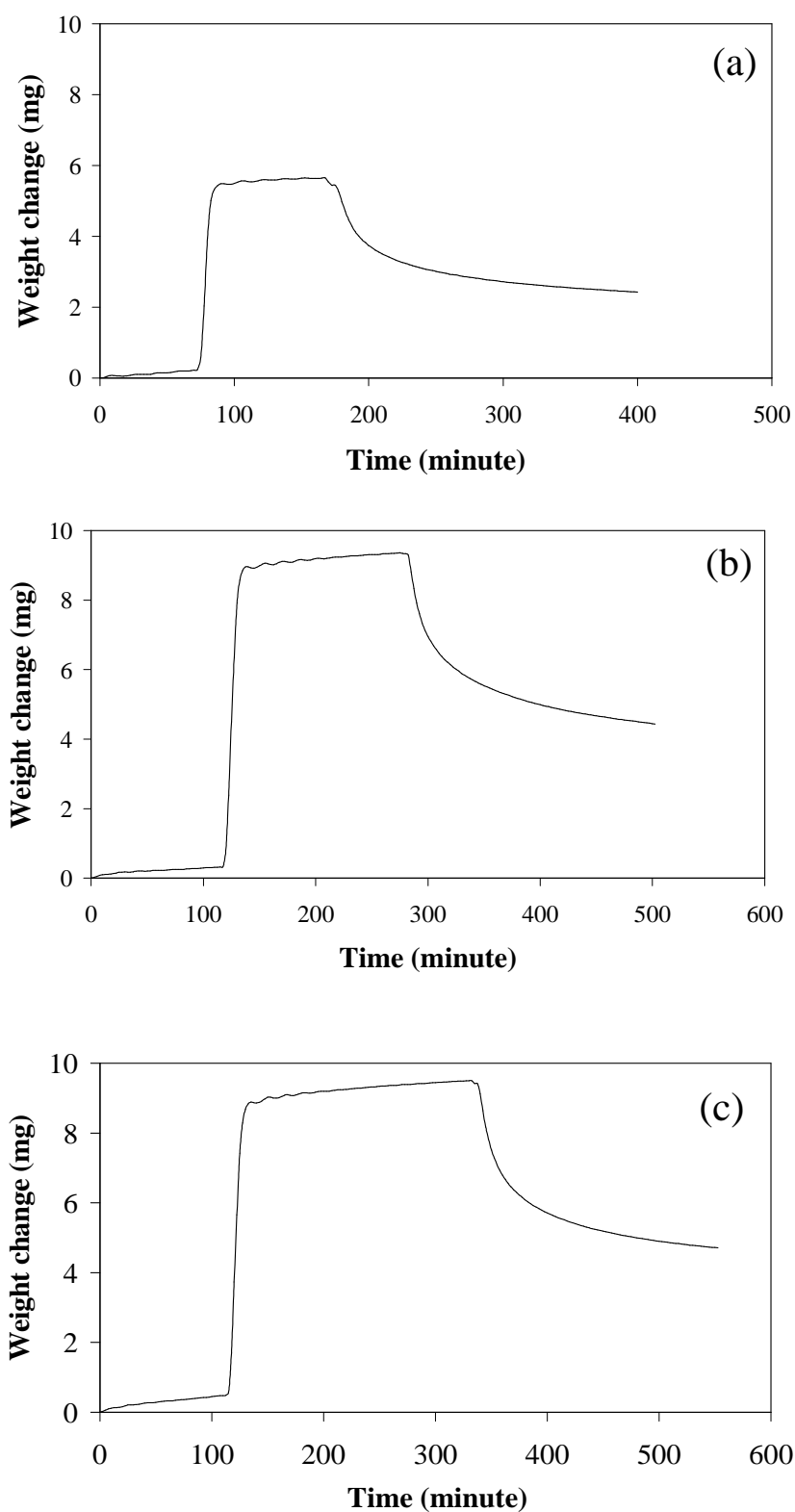
Figure 5.1 Weight changes during ammonia adsorption on (a) RH-MCM-41, (b) RH-

AlMCM-41(75) and (c) RH-AlMCM-41(25).

Table 5.2 Weight change and NH_3 adsorption capacity (mmol/g) of MCM-41 and Al-
MCM-41 from ammonia adsorption

Si/Al ratio	Weight after pretreatment (mg)	adsorbed NH_3 (mg)	NH_3 adsorption capacity (mmol/g)
RH-MCM-41	93.66	2.64	1.66
RH-AlMCM-41(75)	125.19	4.78	2.24
RH-AlMCM-41(25)	123.50	4.55	2.16

Table 5.3 Relative crystallinity, surface area and pore size of RH-MCM-41 and RH-
AlMCM-41

Sample	Relative crystallinity (%)	Surface area (m^2/g)	Pore size (Å)
RH-MCM-41	100	1335	29.2
5Fe0.5Pt /RH-MCM-41	78	-	-
RH-AlMCM-41(75)	89	741	25
5Fe0.5Pt /RH-AlMCM-41(75)	79	-	-
RH-AlMCM-41(25)	68	746	25.7
5Fe0.5Pt/RH-AlMCM-41(25)	57	-	-
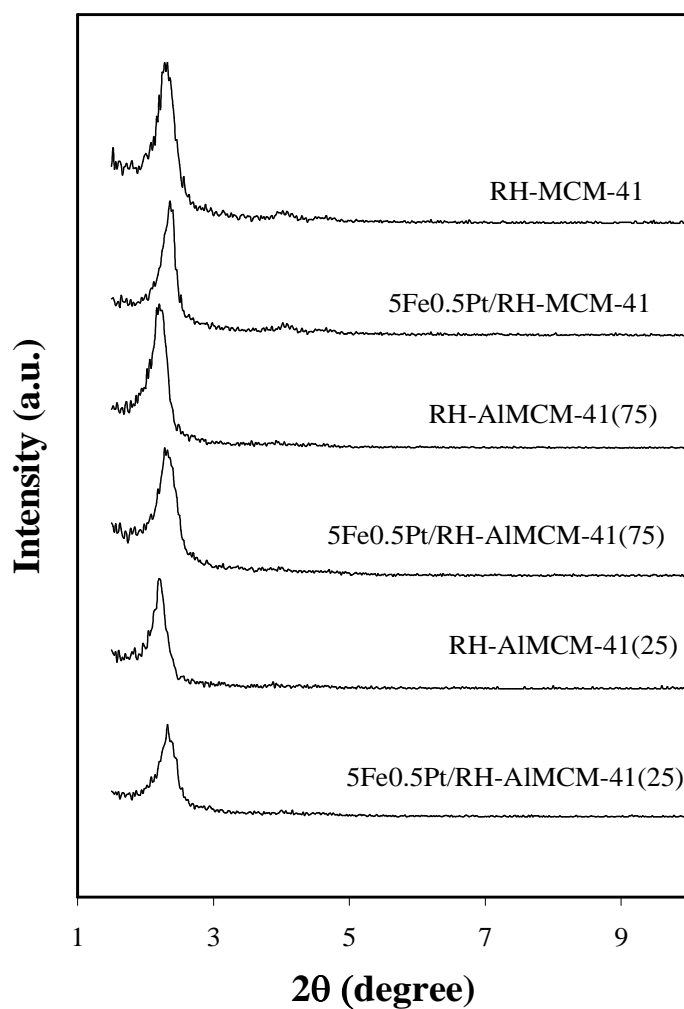
Figure 5.2 XRD patterns of RH-MCM-41, RH-AlMCM-41(75) and RH-AlMCM-41(25) in small angles of all supports and catalysts.
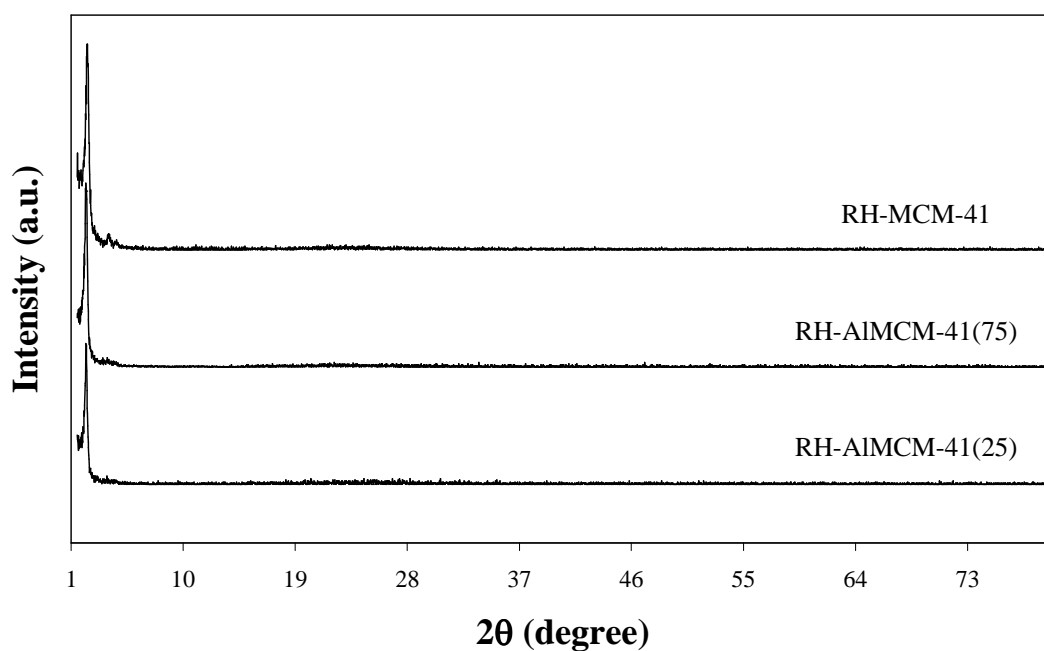
Figure 5.3 XRD patterns of RH-MCM-41, RH-AlMCM-41(75) and RH-AlMCM-41(25) in large angles.

The N_2 adsorption isotherms of RH-MCM-41, RH-AlMCM-41(75) and RH-AlMCM-41(25) samples are shown in Figure 5.4. All isotherms corresponded to a mixture of type IV and type I which are typical isotherms of mesoporous materials. At low P/P_0, the adsorbed amount increased quickly due to adsorption to form monolayer. The adsorbed amounts of all RH-AlMCM-41 samples were lower than that of RH-MCM-41 indicating that their surface areas decreased after Al grafting (see Table 5.3). The N_2 adsorption increased again before reaching a nearly constant volume. This range corresponded to nitrogen adsorption in the mesopores of RH-MCM-41, RH-AlMCM-41(75) and RH-AlMCM-41(25). However, the adsorption in this range for RH-AlMCM-41 did not increased sharply as in RH-MCM-41 indicating

that some mesopores might collapse during the Al-grafting. It was possible that the surface area decreased because the pores of RH-AlMCM-41 were blocked by alumina particles.
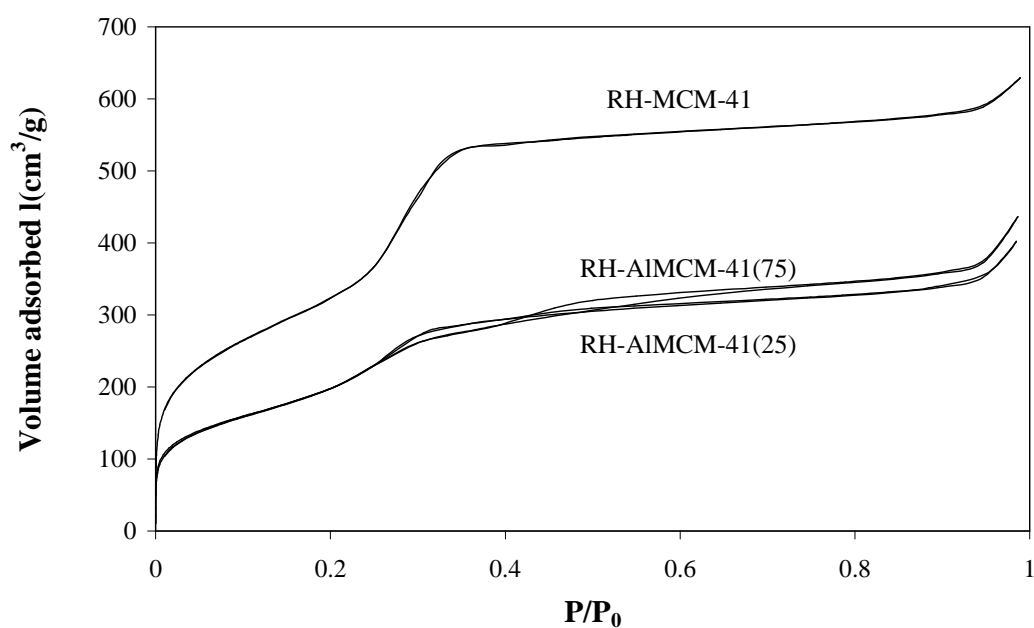
Figure 5.4 N_2 adsorption isotherm of RH-AlMCM-41.
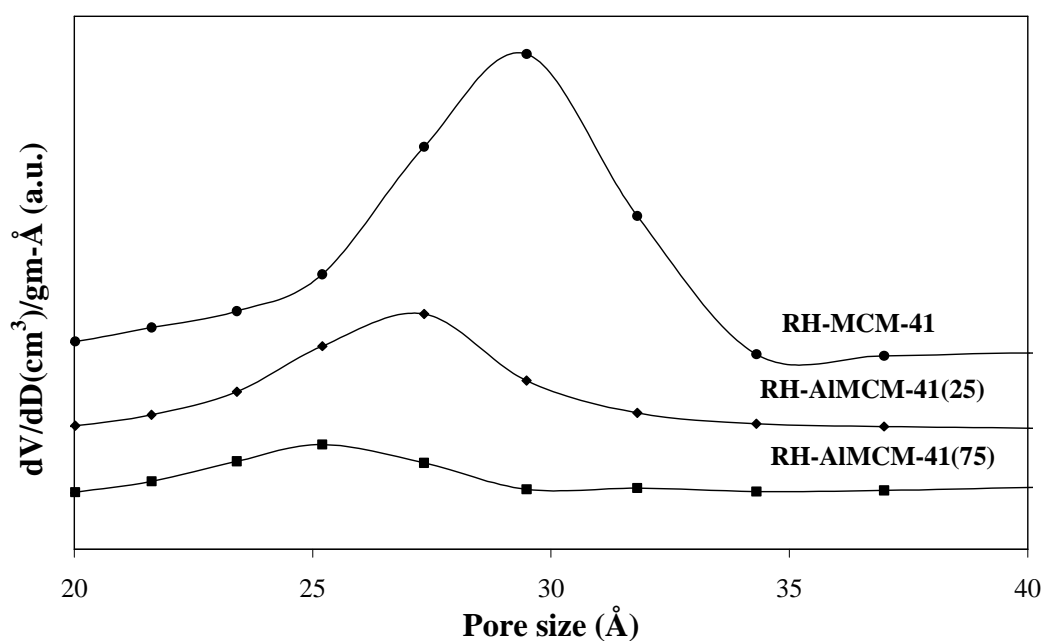
Figure 5.5 Pore size distribution of RH-AlMCM-41.

The TEM images of RH-MCM-41, RH-AlMCM-41(75) and RH-AlMCM-41(25) are shown in Figure 5.7. All samples displayed well-ordered structures.
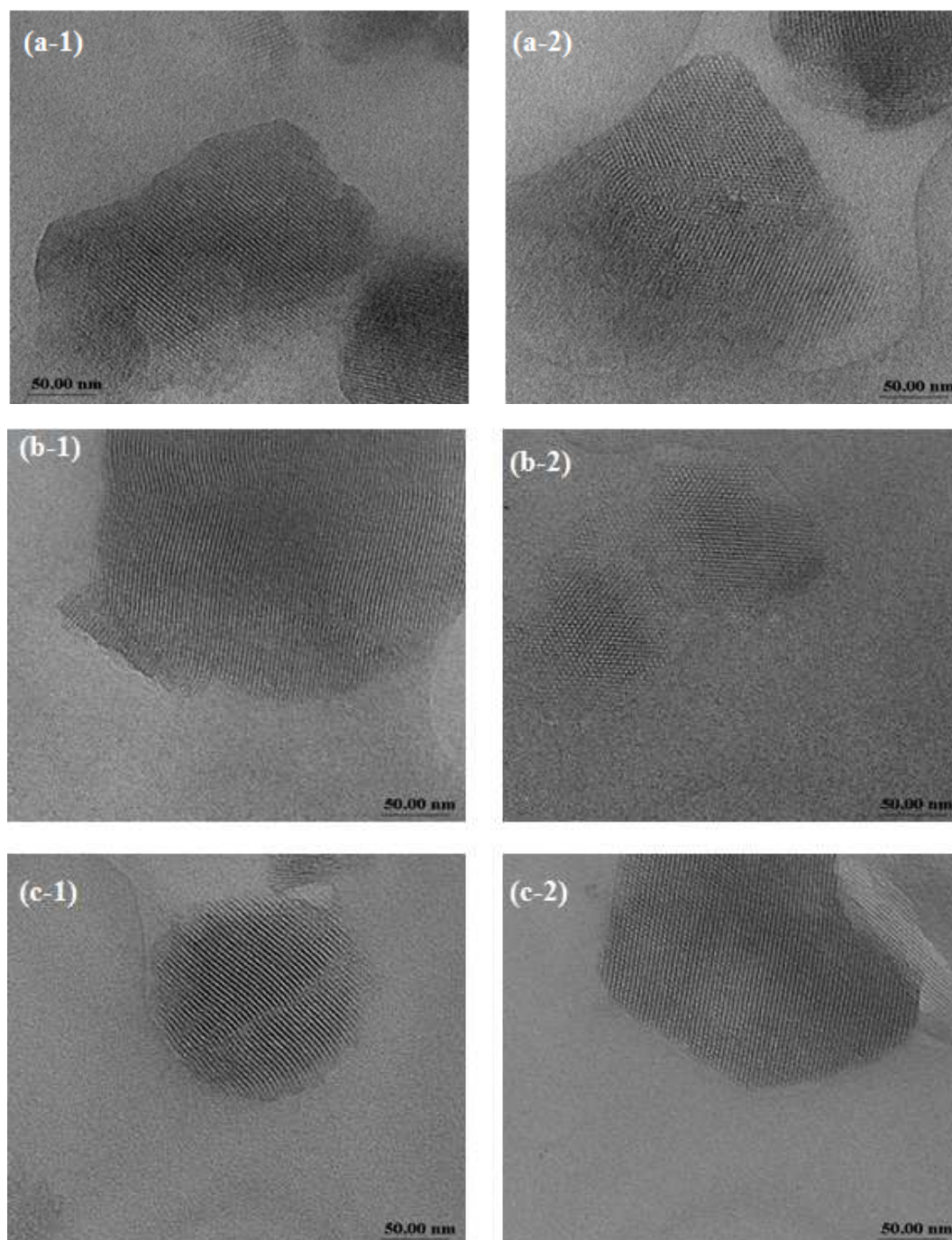
Figure 5.6 TEM micrograph of (a-1and a-2) RH-MCM-41, (b-1 and b-2) RH-Al-MCM-41(75) and (c-1 and c-2) RH-Al-MCM-41(25).

The TPR results from bimetallic Fe-Pt catalysts supported on RH-MCM-41, RH-AlMCM-41(75) and RH-AlMCM-41(25) are shown in Figure 5.7. For 5Fe0.5Pt/RH-MCM-41, there were two peaks, the first peak around 100 °C was assigned to the reduction of platinum and the second around 480 °C was assigned to the reduction of iron. The assignment was based on the fact that platinum oxides are more easily reduced than iron (Jia et al., 1999). For the 5Fe0.5Pt/RH-AlMCM-41(75) and 5Fe0.5Pt/RH-AlMCM-41(25), the reduction peaks of iron in all catalysts shifted to lower temperature with maximum around 380 °C. It was possible that iron on these supports is located near platinum. After platinum oxide was reduced, it may become the adsorption site for hydrogen and the reducer could easily migrate to reduce iron oxides, resulting in lower reduction temperature. Because this behavior was not observed on bimetallic catalyst on RH-MCM-41, it was possible that the presence of Al on RH-MCM-41 created an ion exchange site where Pt(IV) and Fe(III) clustered.

The UV-vis diffuse reflectance spectra in the wavelength range of 200-800 nm of all catalysts are shown in Figure 5.8. A broad band between 220 nm and 250 nm centered at 230 nm, was assigned to the low-energy d_π-p_π charge-transfer transitions between tetrahedral oxygen ligands and central Fe^{3+} ion, was observed for all catalysts. The tetrahedral environment was typical for framework Fe^{3+} ions in Fe-substituted mesoporous molecular sieves. The bands between about 360 and 600 nm were detected, which were corresponding to the Fe species in octahedral coordination Fe_2O_3 crystallites species, respectively. This might be due to the formation of nano-crystalloid Fe_2O_3. (Jia et al., 2007; Wu et al., 2008)
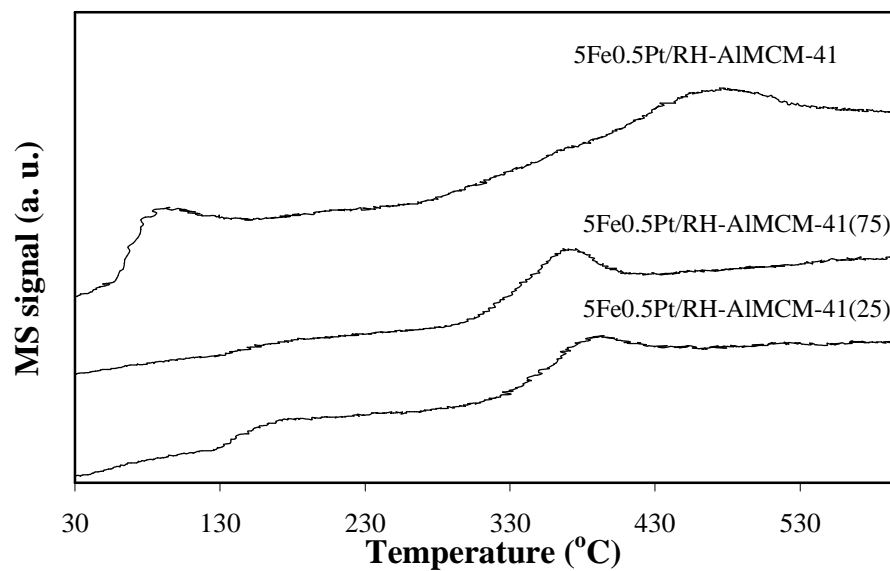
Figure 5.7 Water produced from temperature-programmed reduction of catalysts.
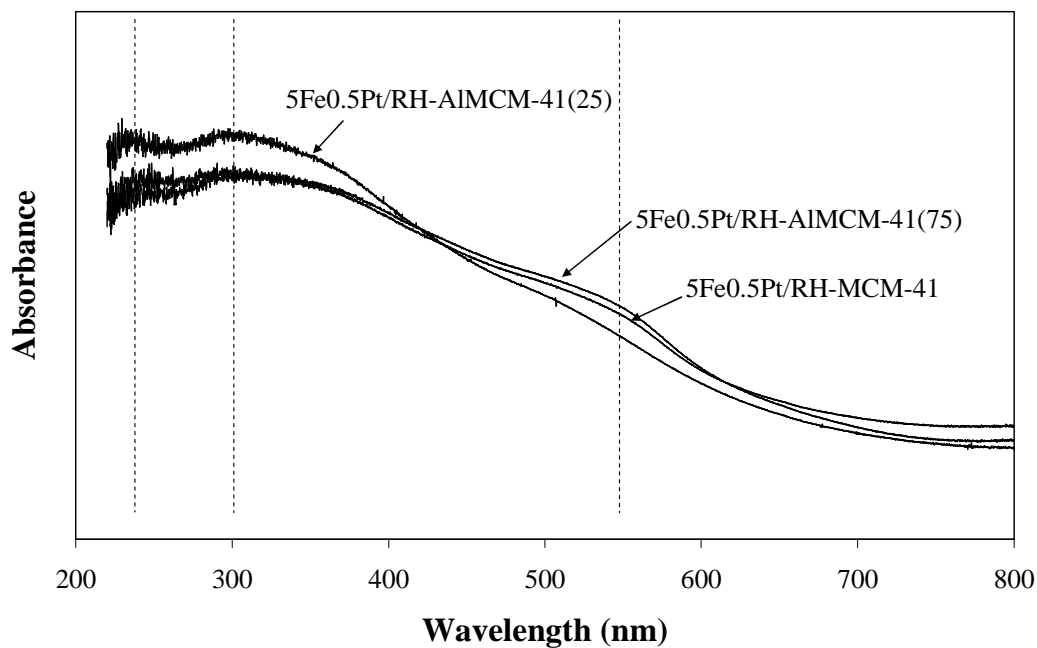
Figure 5.8 UV-vis diffuse reflectance spectra of 5Fe0.5Pt/RH-MCM-41.

Table 5.4 and 5.5 showed the performance of the Fe-Pt bimetallic catalysts for phenol hydroxylation reaction with phenol:H_2O_2 ratios of 3:1 and 2:3. The conversion of phenol increased with the amount of H_2O_2. The conversion was highest at 47% over 5Fe0.5Pt/RH-MCM-41 probably because the support had the highest surface area. After the one hour, all catalysts showed increased of conversion and seemed to approach steady state with a slight increase. As the conversion on 5Fe0.5Pt/RH-AlMCM-41(75) and 5Fe0.5Pt/RH-AlMCM-41(25) were not significantly different, the increase of support acidity did not have a significant influence on the catalytic performance.

Table 5.4 Fe-Pt bimetallic catalysts on RH-AlMCM-41 for phenol hydroxylation (phenol:H_2O_2 = 3:1, 70 °C and amount of catalyst = 0.05 g).

Catalysts	Time (h)	% Conversion of phenol	Selectivity of catechol	Selectivity of hydroquinone
5Fe0.5Pt/RH-MCM-41	1	26.4	49.7	50.3
	2	28.6	48.6	51.4
	3	29.5	50.3	49.7
	4	30.3	49.0	51.0
5Fe0.5Pt/RH-AlMCM-41(75)	1	7.47	71.3	28.7
	2	19.4	49.6	50.4
	3	22.4	48.6	51.4
	4	22.6	48.2	51.8
5Fe0.5Pt/RH-AlMCM-41(25)	1	25.9	48.1	51.9
	2	23.1	49.9	50.1
	3	22.5	47.6	52.4
	4	25.4	46.5	53.5

Table 5.5 Fe-Pt bimetallic catalysts on RH-AlMCM-41 for phenol hydroxylation

(phenol:H_2O_2 = 2:3, 70 °C and amount of catalyst = 0.05 g).

Catalysts	Time (h)	% Conversion of phenol	Selectivity of catechol	Selectivity of hydroquinone
5Fe0.5Pt/RH-MCM-41	0.5	43.6	55.7	44.3
	1	47.6	54.4	45.6
	2	47.3	54.7	45.3
	3	46.6	54.6	46.4
5Fe0.5Pt/RH-AlMCM-41(75)	0.5	37.2	58.0	42.0
	1	46.9	56.7	43.34
	2	45.0	57.5	42.5
	3	46.2	57.5	42.5
5Fe0.5Pt/RH-AlMCM-41(25)	0.5	45.5	54.5	45.5
	1	44.4	56.0	44.0
	2	44.5	54.4	45.6
	3	44.3	53.6	46.4

5.4 Conclusions

RH-MCM-41 was prepared successfully with rice husk silica source and its calculated acidity was improved by adding aluminum via grafting method. However, the aluminum addition caused a decrease in the surface area of RH-AlMCM-41(75) and RH-AlMCM-41(25). The prepared RH-AlMCM-41 materials were used as supports for bimetallic Pt-Fe catalysts and tested for hydroxylation of phenol. However, the 5Fe0.5Pt/RH-MCM-41 showed the highest phenol conversion because the RH-MCM-41 support had significantly higher surface area.

5.5 References

Buurman, P., Vanlagen, B. and Velthorst, J. (1996). **Manual for soil and water analysis**. Backhuys: Netherlands.

Choi, J., Yoon, S., Jang, S. and Ahn, W. (2006). Phenol hydroxylation using Fe-MCM-41 catalysts. **Catalysis Today** 111: 280-287.

Grisdanurak, N., Chiarakorn, S. and Wittayakun, J. (2003). Utilization of mesoporous molecular sieve synthesized from natural source rice husk silica to chlorinated volatile organic compounds (CVOCS) adsorption. **Korean Journal of Chemical Engineering** 20: 950-955.

Huang, S., Jing, S., Wang, J., Wang, Z. and Jin, Y. (2001). Silica white obtained from rice husk in fluidized bed. **Powder Technology** 117: 232-238.

Jia, J., Shen, J., Lin, L., Xu, Z., Zhang, T. and Liang, D. (1999). A study on reduction behaviors of the supported platinum–iron catalysts. **Journal Molecular Catalysis A: Chemical** 138: 177-184.

Jia, Y., Han, W., Xiong, G., and Yang, W. (2007). Diatomite as high performance and environmental friendly catalysts for phenol hydroxylation with H_2O_2. **Science and Technology of Advanced Materials** 8: 106-109.

Jing, H., Guo, Z., Ma, H., Evans D. G. and Duan X. (2002). Enhancing the selectivity of benzene hydroxylation by tailoring the chemical affinity of the MCM-41 catalyst surface for the reactive molecules. **Journal of Catalysis** 212: 22-32.

Park, J.-N., Wang, J., Choi, Y. K., Dong, W.-Y., Hong, S.-I., Lee W. C. (2006). Hydroxylation of phenol with H_2O_2 over Fe^{2+} and/or Co^{2+} ion-exchanged NaY catalyst in the fixed-bed flow reactor. **Journal Molecular Catalysis A: Chemical** 247: 73-79.

Kannan, S., Dubey, A. and Knozinger, H. (2005). Synthesis and characterization of CuMgAl ternary hydrotalcites as catalysts for the hydroxylation of phenol. **Journal of Catalysis** 231: 381-392.

Khemthong, P., Wittayakun, J., Prayoonpokarach, S. (2007). Synthesis and characterization of zeolite LSX from rice husk silica. **Suranaree Journal of Science and Technology** 14: 367-739.

Krishnarao, R. V., Subrahmanyam, J. and Jagadish Kumar T. (2001). Studies on the formation of black particles in rice husk silica ash. **Journal of the European Ceramic Society** 21: 99-104.

Kuznetsova, I. N., Kuznetsova, I. L., Likholobov, A.V. and Pez, P. G. (2005). Hydroxylation of benzene with oxygen and hydrogen over catalysts containing Group VIII metals and heteropoly compounds. **Catalysis Today** 99: 193-198.

Masende, G. P. Z., Kuster, M. F. B., Ptasinski, J. K., Janssen, G. J. J. F., Katima, Y. H. J. and Schouten C. J. (2003). Platinum catalysed wet oxidation of phenol in a stirred slurry reactor; The role of oxygen and phenol loads on reaction pathways. **Catalysis Today** 79-80: 357-370.

Matsumoto, A., Chen H., Tsutsumi, K., Grün, M. and Unger, K. (1999). Novel route in the synthesis of MCM-41 containing framework aluminum and its characterization. **Microporous Mesoporous Materials** 32: 55-62.

Park, K. C., Yim, D. and Ihm, S. (2002). Characteristics of Al-MCM-41 supported Pt catalysts: effect of Al distribution in Al-MCM-41 on its catalytic activity in naphthalene hydrogenation. **Catalysis Today** 74: 281-290.

Shylesh, S. and Singh, P.A. (2004). Synthesis, characterization, and catalytic activity of vanadium-incorporated, -grafted, and -immobilized mesoporous MCM-41 in the oxidation of aromatics. **Journal of Catalysis** 228: 333-346.

Tang, H., Ren, Y., Bin, Y., Yan, S. and He, H. (2006). Cu-incorporated mesoporous materials: Synthesis, characterization and catalytic activity in phenol hydroxylation. **Journal Molecular Catalysis A: Chemical** 260: 121-127.

Wittayakun, J., Khemthong, P. and Prayoonpokrach S. (2008). Synthesis and characterization of zeolite Y from rice husk silica. **Korean Journal of Chemical Engineering** 25: 861-864.

Wu, C., Kong, Y., Gao, F., Wu, Y., Lu, Y., Wang, J. and Dong, L. (2008) Synthesis, characterization and catalytic performance for phenol hydroxylation of Fe-MCM41 with high iron content. **Microporous and Mesoporous Materials** 113: 163-170.

CHAPTER VI

CONCLUSIONS

Rice husk silica prepared by acid leaching was in amorphous phase and had purity of 98 wt%. It was suitable to use as a silica source for the synthesis of RH-MCM-41. The synthesis of RH-MCM-41 by hydrothermal was successful and the obtained product was more stable than that synthesized at ambient conditions which had thinner pore walls. The acidity of RH-MCM-41 was improved by adding aluminum via grafting method. However, the aluminum addition caused a decrease in the surface area of RH-AlMCM-41(75) and RH-AlMCM-41(25). The RH-MCM-41 and RH-AlMCM-41 were used as supported catalyst for Fe-Pt by co-impregnation, the crystallinity and surface area decreased upon metal addition. Metal particles could be observed on RH-MCM-41 and the oxidation state of iron was +3. The catalyst was active for phenol hydroxylation using H_2O_2 as an oxidant when the phenol:H_2O_2 ratios were varied at 2:1, 2:2, 2:3 and 2:4. The first three ratios produced only catechol and hydroquinone whereas the 2:4 ratio produced benzoquinone, thus, the 2:3 ratio was considered to be the most suitable one. The 5Fe0.5Pt/RH-MCM-41 catalyst prepared by co-impregnation from Fe and Pt precursors was more active than a physical mixture of 0.5Pt/RH-MCM-41 and 5Fe/RH-MCM-41. The catalytic performance of 5Fe0.5Pt/RH-MCM-41 was better than that of 5Fe0.5Pt/RH-Silica and 5Fe0.5Pt/RH-AlMCM-41 because the RH-MCM-41 support had a significantly higher surface area than both RH-Silica and RH-AlMCM-41, resulting in a better metal dispersion.

APPENDICES

APPENDIX A

CALIBRATION CURVE OF PRODUCTS AND

REACTANCE FOR PHENOL HYDROXYLATION

Calibration curve of phenol

The calibration curved was prepared by the following procedure. Phenol 0.3030 g was dissolved in 5 mL of ethanol (C = 0.6439 M) and diluted with ethanol to 5 concentrations: C, 1/2C, 1/4C, 1/5C, 1/6C and 0. Then the phenol solutions were analyzed by GC.

The chart shows a calibration curve with the equation:

$$y = (4.4592 \times 10^{12})x$$
$$R^2 = 0.9976$$

where the y-axis is **Peak area** (0 to 200000) and the x-axis is **Mole ($\times 10^{-9}$)** (0 to 40).
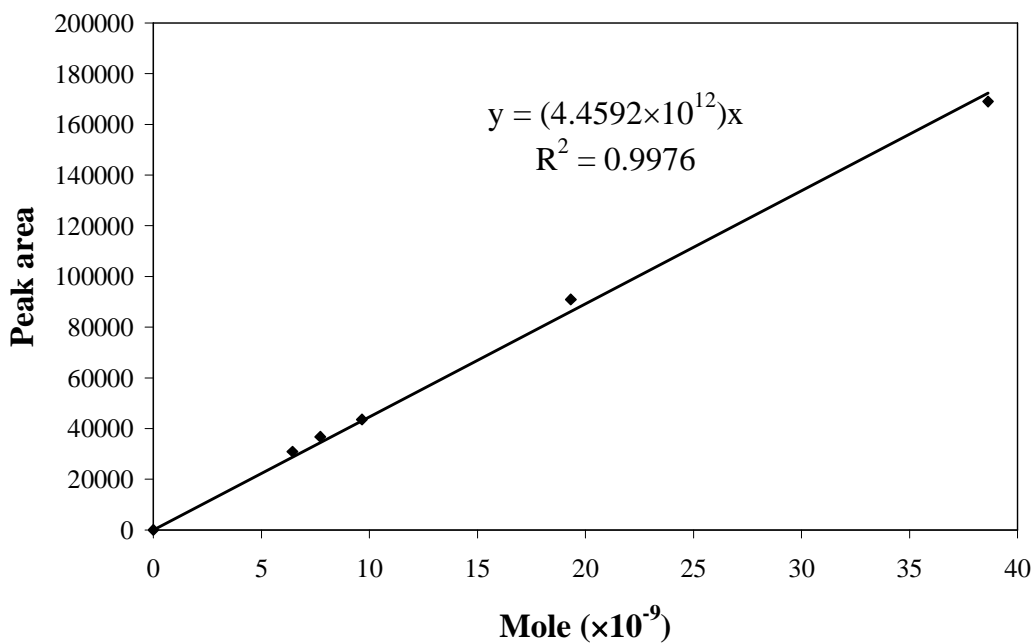
Figure A-1 Calibration curve of phenol for phenol hydroxylation.

88

Calibration curve of catechol

The calibration curved was prepared by the following procedure. Catechol 0.3545 g was dissolved in 5 mL of ethanol (C = 0.6439 M) and diluted with ethanol to 5 concentrations: 1/2C, 1/4C, 1/5C, 1/6C and 0. Then the catechol phenol solutions were analyzed by GC.

The plotted data shows a linear fit with equation:

$$y = (3.2429 \times 10^{12})x$$
$$R^2 = 0.9985$$

with x-axis labeled "Mole ($\times 10^{-9}$)" and y-axis labeled "Peak area".
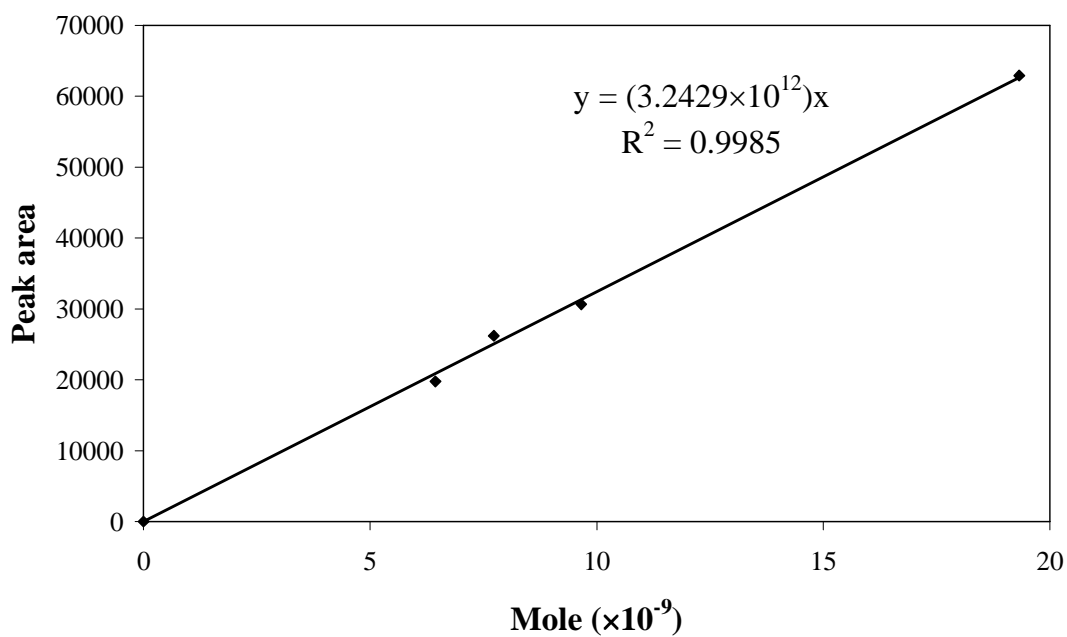
Figure A-2 Calibration curve of catechol for phenol hydroxylation.

Calibration curve of hydroquinone

The calibration curved was prepared by the following procedure. Hydroquinone 0.3548 g was dissolved in 5 mL of ethanol (C = 0.6439 M) and diluted with ethanol to 5 concentrations: 1/2C, 1/4C, 1/5C, 1/6C and 0. Then the hydroquinone phenol solutions were analyzed by GC.

$$y = (2.3342 \text{Mole}(\times 10^{12})x$$
$$R^2 = 0.9948$$
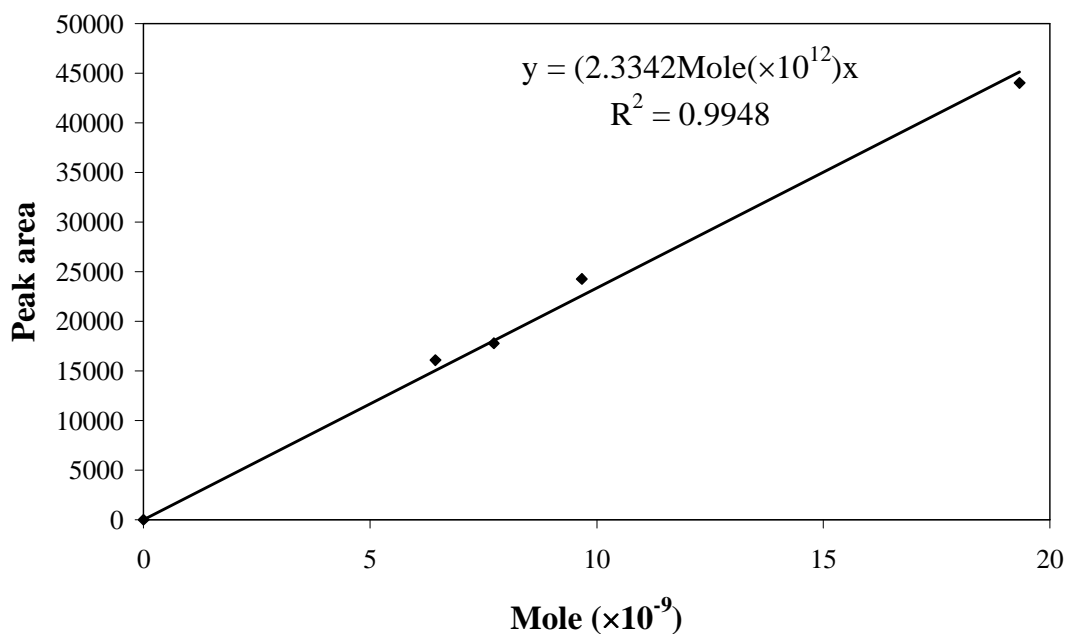
Figure A-2 Calibration curve of hydroquinone for phenol hydroxylation.

Calculation for phenol conversion

The conversion was calculated as follows;

$$X_{\text{PhOH}}\ (\%) = 100 \times ([\text{PhOH}]_i - [\text{PhOH}]_f)/\ [\text{PhOH}]_i$$

where

X_{PhOH} is the conversion of phenol

$[\text{PhOH}]_i$ is the mole of phenol before reaction

$[\text{PhOH}]_f$ is the mole of phenol after sampling

PhOH_f was calculated as follows;

$$y = 4.4592 \times 10^{12} x$$

y = peak area of phenol after sampling

x = mole of phenol after sampling

PhOH_I was calculated as follows;

$$\text{PhOH}_I = g/\text{MW}$$

Where

g   = Weight of phenol before reaction

MW = Molecular Weight of phenol (94.11 g/mole)

Calculation of product selectivity

The selectivity was calculated as follows:

Product selectivity (%) = $100 \times [\text{product}]_f/([\text{CAT}]_f + [\text{HQ}]_f + [\text{BQ}]_f + [\text{BPs}]_f)$,

where

$[\text{product}]_f$ is the molar concentration of catechol, hydroquinone,

benzoquinone and the by-products, after the reaction.

APPENDIX B

DATA FROM N$_2$ ADSORPTION-DESORPTION

Table B-1 N$_2$ adsorption-desorption of RH-MCM-41.

P/P$_0$	Volume adsorbed	P/P$_0$	Volume adsorbed
0.000015161	10.1389	0.450022245	498.6141
0.000018331	20.2834	0.500966820	503.1909
0.000020356	30.4288	0.551142653	507.2536
0.000024909	40.573	0.601184134	511.0133
0.000034611	50.7151	0.651543871	514.577
0.000051917	60.854	0.700091751	517.9923
0.000080546	70.9884	0.759203106	527.3678
0.000125890	81.1161	0.811309385	532.7388
0.000197041	91.2338	0.848429511	535.2161
0.000308163	101.336	0.902458887	543.1802
0.000478999	111.3848	0.947267328	556.9137
0.000738023	121.4291	0.987539297	631.7742
0.001121168	131.4234	0.949384919	561.5743
0.002997893	156.6317	0.888951777	541.7089
0.004793144	169.674	0.842102575	534.9941
0.006705246	179.4966	0.789467892	529.8355
0.008762671	187.804	0.752414919	526.7435
0.009678527	190.9029	0.700255565	522.7948
0.015038124	205.5513	0.649999062	519.1815
0.020076602	215.6821	0.599959628	515.6057
0.024146481	222.5119	0.549967674	511.8733
0.028976388	229.5543	0.499883924	507.8362
0.034476244	236.5531	0.45075887	502.8045
0.039906577	242.7289	0.400447711	495.9921
0.044960856	247.9393	0.346732494	489.1594
0.049962842	252.759	0.302709055	481.9224
0.055097693	257.3738	0.254383295	435.457
0.058128649	259.9784	0.202497765	360.8479
0.065033724	265.5876	0.146961091	320.2275
0.069985609	269.4153	0.098324471	289.5517
0.074932260	273.0916	0.094177354	286.8108
0.079863228	276.6318	0.079855068	276.9593
0.084765228	280.043	0.070045665	269.7218
0.089694198	283.4203	0.060017937	261.6739
0.094601549	286.6847	0.050688951	253.4762
0.099549338	289.9291	0.040292867	243.0298
0.145442936	318.4155	0.031099452	232.1582
0.203387045	359.8584	0.020913973	216.6684
0.246623783	417.3768	0.010498963	192.6028
0.310584929	481.6978		
0.371269621	490.2229		
0.412340722	494.8371		

Table B-2 N_2 adsorption-desorption of 5Fe/RH-MCM-41.

P/P_0	Volume adsorbed	P/P_0	Volume adsorbed
0.000015003	10.1477	0.550182	318.4168
0.000021142	20.2990	0.599911	321.0972
0.000030436	30.4486	0.649817	323.6300
0.000050015	40.5931	0.699718	326.1159
0.000090258	50.7292	0.749671	328.6680
0.00016979	60.8493	0.799392	331.6030
0.000324808	70.9374	0.849695	334.9993
0.000616507	80.9918	0.898041	339.8448
0.001146966	90.9506	0.945454	349.3110
0.002851261	106.5899	0.983838	383.8804
0.004883988	116.5974	0.951740	354.6111
0.00669	122.7186	0.892315	347.2591
0.00878	128.3448	0.847789	336.8835
0.009677	130.4173	0.797383	333.3121
0.015373	140.5963	0.736595	329.9092
0.019272	145.9395	0.700981	328.2441
0.024522	151.8658	0.651047	325.7974
0.029864	156.9806	0.599754	323.3956
0.034862	161.1984	0.550336	321.0802
0.039972	165.0926	0.500327	318.6138
0.045018	168.6158	0.45169	315.0743
0.050089	171.9043	0.400629	309.7732
0.053404	173.9319	0.348368	305.2975
0.059919	177.7396	0.302808	300.4777
0.064972	180.5667	0.254781	279.8747
0.06994	183.2158	0.205855	246.0332
0.074791	185.7182	0.148082	219.1044
0.079786	188.1958	0.101067	198.7216
0.084701	190.5547	0.091806	194.4844
0.089587	192.8742	0.080154	188.9212
0.094485	195.1595	0.070172	183.887
0.099498	197.4426	0.060259	178.5161
0.146602	217.7859	0.05024	172.5664
0.195217	239.5519	0.04051	165.9801
0.250666	275.3932	0.030407	157.9432
0.312458	300.8278	0.020761	148.1159
0.346259	304.1889	0.010251	131.7933
0.41102	309.4086		
0.448932	312.0949		
0.499778	315.4288		

Table B-3 N$_2$ adsorption-desorption of 0.5Pt/RH-MCM-41.

P/P$_0$	Volume adsorbed	P/P$_0$	Volume adsorbed
0.00003106	10.6492	0.50542918	476.0800
0.00004264	21.3033	0.54760091	479.8303
5.7645E-05	31.9481	0.59946565	483.9177
8.2199E-05	42.5966	0.64957825	487.476
0.00012499	53.2395	0.69927327	490.8492
0.00019968	63.8700	0.74932279	494.2580
0.00032617	74.4776	0.79910865	497.8893
0.00053331	85.0487	0.84855114	502.1699
0.00086922	95.5591	0.89741566	508.0517
0.00139003	105.987	0.94286298	518.6034
0.00285297	122.5795	0.98612408	568.8307
0.00475691	134.8916	0.95654845	528.1790
0.00671144	143.2121	0.90258974	509.6668
0.00856693	149.7148	0.84974349	502.5809
0.00973471	153.1153	0.79400075	497.8242
0.01494752	165.1889	0.7557066	494.9991
0.01966782	173.3519	0.70137778	491.4867
0.02419869	179.8694	0.65186331	488.4391
0.02976496	186.7487	0.60152288	485.2739
0.03411043	191.4801	0.55142665	481.8864
0.03927881	196.6217	0.50135161	478.1325
0.04486273	201.644	0.45248829	473.1053
0.04993768	205.8575	0.40412004	464.7931
0.05495213	209.7761	0.34532319	454.3427
0.05773728	211.8457	0.30162067	388.7971
0.06485600	216.8931	0.24755467	312.8165
0.06986581	220.2727	0.2065335	290.6402
0.07479473	223.4466	0.14860286	263.5029
0.07969937	226.4869	0.1023067	239.8416
0.08463061	229.4546	0.0895914	232.676
0.08958806	232.3813	0.07984535	226.9102
0.09451571	235.1966	0.07045093	220.9010
0.09945893	237.9491	0.06043305	214.0040
0.14635088	262.0147	0.05234384	207.8886
0.19696642	286.1978	0.04080477	198.0761
0.24606704	311.6378	0.0305569	187.6621
0.29475727	370.5047		
0.35707545	457.5617		
0.45232472	470.6018		

Table B-4 N_2 adsorption-desorption of 5Fe0.5Pt/RH-MCM-41.

P/P$_0$	Volume adsorbed	P/P$_0$	Volume adsorbed
0.00002115	10.9911	0.499734707	362.3972
0.000029946	21.9863	0.549615169	366.8276
0.000041564	32.9793	0.599606031	371.0874
0.000063581	43.9646	0.649600478	375.1839
0.00010874	54.9366	0.699532617	379.1204
0.00019874	65.8818	0.749368578	382.9423
0.000378512	76.7752	0.799185686	386.8029
0.000725352	87.5714	0.849561907	391.1795
0.001348851	98.1679	0.898475851	397.0947
0.00287046	111.8633	0.944858806	408.2547
0.00483966	121.9387	0.985684088	464.5727
0.006741173	128.5741	0.951479788	423.0921
0.008786053	134.255	0.89595062	399.8069
0.009588587	136.2231	0.843436506	392.8734
0.015077708	146.6464	0.789601371	388.1979
0.019670586	153.2508	0.753346476	385.5118
0.024420849	158.8844	0.700993359	381.9702
0.029773845	164.3372	0.651078791	378.5579
0.03490366	168.9072	0.600930988	374.8398
0.039952897	172.9625	0.550222255	370.9452
0.045036315	176.7108	0.5006035	366.9724
0.050065835	180.1859	0.452886937	361.5349
0.053218759	182.2903	0.401351039	353.4681
0.060076115	186.4706	0.344761496	346.752
0.064958747	189.3379	0.305416849	341.0666
0.069861774	192.0928	0.247193187	303.4286
0.074757704	194.7445	0.197189663	258.3038
0.07968109	197.3349	0.147884951	230.416
0.084639672	199.8763	0.100947413	208.2854
0.089512725	202.3107	0.094406448	205.1367
0.094393181	204.7498	0.080210868	198.0598
0.09932413	207.0931	0.070230325	192.7505
0.145402592	228.755	0.06019274	187.0179
0.203539868	262.1015	0.050258404	180.7843
0.243877239	298.4621	0.041282035	174.4428
0.293699009	337.7355	0.030427784	165.3782
0.372231622	349.5841	0.020807342	154.9569
0.411720055	353.9067	0.010242791	137.6993
0.447982114	357.5597		

Table B-5 N_2 adsorption-desorption of RH-AlMCM-41(75).

P/P_0	Volume adsorbed	P/P_0	Volume adsorbed
0.000013706	10.1252	0.497711107	306.2316
0.000021191	20.2536	0.547241732	314.8225
0.000040493	30.3782	0.597418421	322.8061
0.000090748	40.4927	0.647565361	329.7434
0.0002109	50.5813	0.697121892	335.3808
0.000484943	60.619	0.745882175	340.1811
0.001067471	70.5472	0.79558965	344.7842
0.002880471	84.2453	0.844760871	349.9454
0.004876729	92.1963	0.89426155	357.0479
0.00672965	97.2094	0.946436366	372.2951
0.008771957	101.6981	0.986308671	436.5214
0.009659007	103.3785	0.948284806	376.8154
0.015317705	111.7559	0.907111604	361.2123
0.019282883	116.2028	0.846603516	351.4335
0.02429399	120.8657	0.789003878	345.7703
0.029718327	125.1701	0.752818841	342.6801
0.03472347	128.6514	0.698374092	338.5956
0.039758019	131.8067	0.649183588	334.9468
0.044795533	134.7114	0.599251223	330.9042
0.049837395	137.4008	0.549754409	326.0667
0.054803146	139.8711	0.499591511	320.0824
0.058181795	141.4905	0.456452275	309.4428
0.064639116	144.4313	0.388665648	284.4718
0.069588923	146.5817	0.333768218	271.2906
0.074635737	148.7095	0.294289414	258.5419
0.07955411	150.7114	0.24756317	227.8275
0.084548432	152.6955	0.203742169	199.1698
0.089387988	154.5806	0.14870994	175.516
0.09436243	156.459	0.100826786	158.2103
0.099311608	158.2997	0.093710605	155.5415
0.145759089	175.0468	0.080527949	150.4458
0.204490446	200.0172	0.070495152	146.3516
0.246363687	227.0792	0.06010614	141.7832
0.305230868	263.2779	0.050619547	137.1984
0.365316492	279.4166	0.040794889	131.8013
0.401313303	287.4211	0.030380823	125.0236
0.446096701	296.5774	0.020030317	116.2772
0.010133865	103.3904		

Table B-6 N_2 adsorption-desorption of RH-AlMCM-41(25).

P/P_0	Volume adsorbed	P/P_0	Volume adsorbed
0.000019282	10.7829	0.358345877	287.5055
0.000027813	21.5697	0.403528156	294.2625
0.000042356	32.3531	0.454393335	300.3758
0.000080698	43.124	0.496329391	304.6477
0.000178506	53.8658	0.546619283	309.062
0.000421375	64.539	0.596402584	312.9147
0.000987267	75.0567	0.646139235	316.4179
0.002170251	85.2966	0.695764079	319.7911
0.002891001	89.2657	0.745607447	323.2357
0.00482133	96.5061	0.795313035	326.9576
0.006840808	101.6121	0.844520969	331.4994
0.008818464	105.6566	0.894019572	337.8055
0.009722254	107.2369	0.945457944	351.3418
0.015256819	114.8509	0.984631926	401.9095
0.019428769	119.2152	0.95028973	357.5015
0.02437784	123.5306	0.884649194	337.6411
0.029753533	127.5272	0.837980689	331.8943
0.03481819	130.8448	0.785916757	327.4238
0.039846249	133.8341	0.749145828	324.8138
0.044922401	136.5982	0.697855334	321.5387
0.049915578	139.1307	0.647749645	318.5429
0.05496079	141.5467	0.597979082	315.5735
0.058348631	143.1031	0.547964664	312.5246
0.064828239	145.9144	0.498751869	309.0865
0.069828139	147.9973	0.451929503	303.3222
0.074733342	149.963	0.399994316	293.9507
0.079614467	151.8835	0.34340545	284.7525
0.084557054	153.7533	0.306288438	274.9793
0.089436474	155.5747	0.250327097	230.4067
0.094389982	157.3959	0.206200163	200.8293
0.099277421	159.1461	0.14826219	176.0908
0.14577149	175.4046	0.100502507	159.2553
0.204548609	200.0067	0.094078415	156.9016
0.246361922	226.8543	0.08028591	151.7512
0.294646993	268.159		

APPENDIX C

THESIS OUTPUT

1. Chumee, J., Grisdanurak, N., Neramittagapong A., and Wittayakun, J., Characterization of platinum-iron catalysts supported on MCM-41 synthesized with rice husk silica and their performance for phenol hydroxylation, *Science and Technology of Advanced Materials*, 10 (2009) 015006.

2. Chumee, J., Grisdanurak, N., Neramittagapong S. and Wittayakun J., Characterization of AlMCM-41 synthesized with rice husk silica and utilization as supports for platinum-iron catalysts, *Brazil Journal of Chemical Engineering*, 26(2) (2009) pp. Accepted on 2 December 2008.

CURRICULUM VITAE

JITLADA CHUMEE

Gender: Female

Birth date: 30 March 1981

Address: 1/4 Soi Chayangkul 42.2, Chayangkul road, Tambon Nai Mueang, Amphoe Muang, Ubolratchathani, 34000, Thailand

Email: sugar_cans@hotmail.com

Education:

    2000-2004   B. Sc. (Chemistry) Ubon Rajathani University, Thailand

    2004-2008   Ph. D. (Chemistry) Suranaree University of Technology, Thailand

International Papers:

J. Chumee, N. Grisdanurak, A. Neramittagapong and J. Wittayakun, Characterization of platinum-iron catalysts supported on MCM-41 synthesized with rice husk silica and their performance for phenol hydroxylation, Science and Technology of Advanced Materials, 10 (2009) 015006.

J. Chumee, N. Grisdanurak, S. Neramittagapong and J. Wittayakun, Characterization of AlMCM-41 synthesized with rice husk silica and utilization as supports for platinum-iron catalysts, Brazil Journal of Chemical Engineering, accepted.